

**Aminoacid Grafted Chitosan Polymers -Synthesis and
Characterization**

**REEBA.N
(21PCH018)**

**Thesis submitted to
Avinashilingam Institute for Home Science and Higher Education for
Women,
Coimbatore- 641043.**

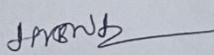
**In Partial Fulfilment
of the Requirements for the Degree of
MASTER OF SCIENCE IN CHEMISTRY
May-2023**

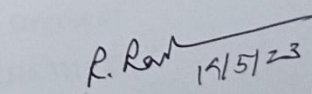
**Aminoacid Grafted Chitosan Polymers -Synthesis and
Characterization**

**REEBA.N
(21PCH018)**

**Thesis submitted to
Avinashilingam Institute for Home Science and Higher Education for Women,
Coimbatore- 641043.**

**In Partial Fulfillment of the Requirements for the Degree of
MASTER OF SCIENCE IN CHEMISTRY
MAY - 2023**


**Signature of the
Supervisor**


**Signature of the
Head of the Department**



ACKNOWLEDGEMENT

Firstly I would like to thank Mahadev for letting me through all the difficulties and hardships which led to the successful completion of my thesis in serene

I express my profound thanks to **Prof. S.P. Thyagarajan**, Chancellor, Avinashilingam Institute for Home Science and Higher Education for Women, Coimbatore, for providing a learning opportunity in this university.

I owe my sincere thanks to **Dr. V. Bharathi Harishankar** Vice Chancellor, Avinashilingam Institute for Home Science and Higher Education for Women, Coimbatore, providing opportunity to develop and establish my skills

I am indebted to **Dr. Mrs. S. Kowsalya**, Registrar, Avinashilingam Institute for Home Science and Higher Education for Women, Coimbatore, for supporting me directly or indirectly for the fulfilment of the thesis

My heartfelt thanks go to **Dr. P. Lalitha** (Research and Consultancy), Avinashilingam Institute for Home Science and Higher Education for Women, Coimbatore, who have provided me their valuable support and insight throughout my project

I would like to expand my deepest gratitude to **Dr. (Mrs.) G. Padmavathi** Dean, Faculty of Science, Avinashilingam Institute for Home Science and Higher Education for Women, Coimbatore, for making all necessary arrangements during the course of the work.

My immense thanks goes to **Dr. (Mrs.) R. Saratha**, Professor and Head, Department of Chemistry, Avinashilingam Institute for Home Science and Higher Education for Women, Coimbatore, for providing the entire facilities for the successful completion of the project.

I owe my deep sense of gratitude to my guide, **Dr.V.Sharulatha** , Associate Professor, Department of Chemistry, Avinashilingam Institute for Home Science and Higher Education for Women, for the unending source of inspiration. Her constant guidance and willingness of sharing her knowledge were unstoppable.

I am much obliged to thank all my staff members and lab technicians in the Department of Chemistry for extending their support, and consistent encouragement.

I am overwhelmed to thank my Ph.D. research scholars Kiruthuka S and Keerthana L the Department of Chemistry, and friends Akshaya L, and Nandhini M who helped a lot in finalizing this thesis within the limited time frame.

I am forever thankful to my family members for their unconditional love and kindness throughout my lifetime

REEBA.N



TABLE OF CONTENTS

CONTENTS

S.No	CHAPTER	Pg.No
	LIST OF ABBREVIATION	
	LIST OF TABLE	
	LIST OF FIGURES	
1	INTRODUCTION	2
2	REVIEW OF LITERATURE	14
3	MATERIALS AND METHODS	24
4	RESULTS AND DISCUSSION	27
5	SUMMARY AND CONCLUSION	48
6	REFERENCES	50

LIST OF ABBREVIATION

CS	Chitosan
LTHR	L-Threonine
LHP	L-Hydroxy proline
LTHR &LHP	Threonine &Hydroxy Proline
LTHR-g-CS	L-Threonine grafted Chitosan
LHP-g-CS	L-Hydroxy proline grafted Chitosan
LTHR &LHP -g-CS	L-Threonine & L-Hydroxy Proline grafted Chitosan
FT-IR	Fourier Transfer Infrared Spectroscopy
TGA	Thermal Gravimetric Analysis
SEM	Scanning Electron Microscope
HEMA	2-Hydroxy Ethyl Methacrylate

LIST OF TABLES

TABLE NUMBER	NAME OF TABLE	PAGE NUMBER
01	The yields of product formed	30

LIST OF FIGURES

FIGURE NUMBER	NAME OF FIGURE	PAGE NUMBER
1	FT-IR spectrum of L- Threonine grafted chitosan	31
2	FT-IR spectrum of L-Hydroxy proline grafted chitosan	32
3	FT-IR spectrum of L-Threonine and L- Hydroxy proline grafted chitosan	33
4	DTA of L- Threonine grafted chitosan	34
5	TGA of L- Threonine grafted chitosan	35
6	Weight loss graph of L- Threonine grafted chitosan	35
7	DTA of L-Hydroxy proline grafted chitosan	36
8	TGA of L-Hydroxy proline grafted chitosan	37
9	Weight loss graph of L-Hydroxy proline grafted chitosan	37
10	DTA of Threonine and Hydroxy proline grafted chitosan	38
11	TGA of Threonine and Hydroxy proline grafted chitosan	39
12	Weight loss graph of Threonine and Hydroxy proline grafted chitosan	39

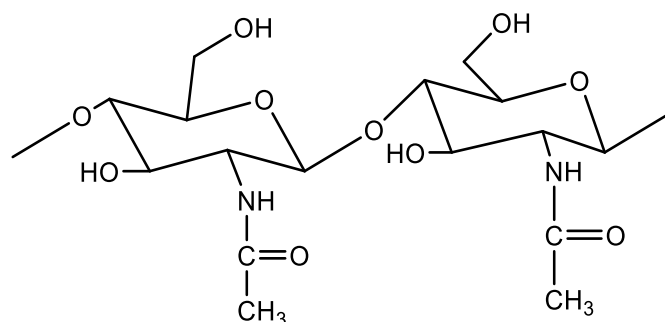
13	TGA curve of amino acid grafted chitosan	40
14	DTA curve of amino acid grafted chitosan	41
15	SEM image of 316L stainless steel without coating	43
16	SEM image of 316L stainless steel coated with L-THR-g-CS using polyethylene glycol	43
17	SEM image of 316L stainless steel coated with LHP-g-CS using polyethylene glycol	44
18	SEM image of 316L stainless steel coated with LTHRLHP-g-CS using polyethylene glycol	44
19	SEM image of 316L stainless steel coated with L-THR-g-CS using glycerol	45
20	SEM image of 316L stainless steel coated with L-THR-g-CS using Poly-2-hydroxyethyl methacrylate	45
21	SEM image of 316L stainless steel coated with LHP-g-CS using polyethylene glycol at PH =6.1	46
22	SEM image of 316L stainless steel coated with LHP-g-CS using polyethylene glycol at PH=3.4	46



1. INTRODUCTION

CHITIN

Chitin, a mucopolysaccharide occurs naturally in abundance and is white, hard, inelastic, and nitrogenous and is a by-product of the fishing industry, is regarded as a renewing raw resource and is only second to cellulose in terms of abundance. (Islam *et al.*,2016) .As a component of the cell walls and structural membranes of mycelia, stalks, and spores, chitin is found in a wide variety of species throughout the Mycota Kingdom, including Ascomycetes, Zygomycetes, Basidiomycetes, and Phycomycetes. Chitin levels are often greater in the Zygomycetes class. (Kaur *et al.*,2013)



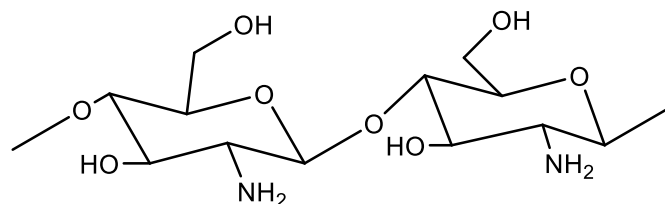
Chitin is a poly ((1-4)-N-acetyl-D-glucosamine) with (1-4) links that are thought to have a cellulose-like structure with an acetamido group in the C2 position. Chitin exhibits three polymorphs

indicated as α , β and γ and, depending on the orientation of polysaccharide chains. The α -type is the one that is most prevalent in shellfish. This polymorph features an antiparallel structure in which each chain strongly interacts with the neighbouring one through hydrogen bonds, resulting in great thermochemical stability and high insolubility. As a result, chitin is a polymer that is very difficult to dissolve and is therefore not biodegradable. Hence, only the widely present chitinase enzymes in nature can break down chitin. Its usefulness is restricted by its low solubility in water and most organic solvents **(Iménez-Gómez *et al.*,2020)**

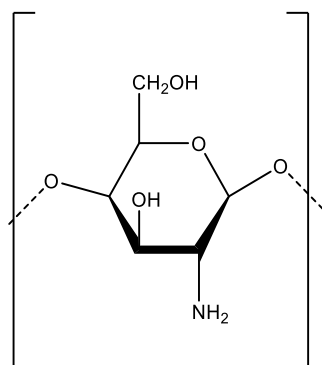
The cell walls of some other microorganisms, including fungi and algae, as well as crustaceans include chitin. Chitin is produced by plants at a rate that is almost 10 Gtons (1 1013 kg) each year The main variation between the chemical structures of chitin and cellulose is that chitin has an acetamido group instead of cellulose's hydroxyl group in the C-2 position. **(Kaur *et al.*,2013)**

CHITOSAN

Rouget developed chitosan in 1859 by heating chitin in an alkaline solution. Hoppe-Seyer gave this substance the name "chitosan" a few years later, despite the fact that its chemical makeup was not fully understood until 1950. **(Carmen *et al.*,2020)**



Chitosan is weakly basic ($pK_a = 6.3$) because it contains amine groups, and is highly soluble in acidic solutions (mostly below $pH = 6.0$). Because of the protonation of the amine groups at low pH levels, chitosan can act as a water-soluble cationic polyelectrolyte. The biopolymer loses its elasticity and becomes an insoluble polymer as the pH rises beyond 6, though, since the amine groups of chitosan residues are deprotonated. **(Carmen *et al.*,2020)**



Chitosan is a naturally occurring polysaccharide that can be used for tissue engineering and medication administration. It is cationic, very basic, mucoadhesive, and biocompatible. Chitin from natural sources is typically found attached to proteins and minerals, which need to be freed prior to the production of chitosan using acidification and alkalization methods. Afterward, purified chitin is N-deacetylated to produce chitosan. (Mohammed *et al.*,2017)

Due to its high molecular weight and little shelf life, chitosan has a limited range of uses because it is less soluble. The varying viscosities (2000 mPa.s.), levels of deacetylation (48%-98%), and molecular weights are displayed by the series of chitosan polymers (50 kDa–2000 kDa). Chitosan has advantageous properties such as being non-toxic, biocompatible, biodegradable, and non-carcinogenic. Chitosan hence has potential use in a variety of industries, including biomedicine, as an antibacterial agent, wastewater treatment, food packaging, functional membranes, and d5flocculation. (Kumar *et al.*,2020)

Application

Materials derived from nature are needed for one of the current developments in implantable applications. First off, studies on such "natural" materials have revealed that they better encourage healing at a faster rate and are predicted to be more tolerant of people. Second, novel ideas for implanted medical devices, particularly tissue engineering made of a combination of biomaterials onto which cells are seeded, need "temporal" aspects that require the biomaterial to be biodegradable into non-toxic by-products (Khor *et al.*,2003)

Phosphorus elemental analysis, IR, and ³¹P-NMR spectroscopy were used to describe the water-soluble phosphorylated chitosan (P-chitosan) that was produced after chitosan was phosphorylated by P₂O₅ in methane sulfonic acid. Various water-soluble P-chitosan with different molecular weights, degrees of deacetylation (DD), and degrees of substitution were added to monocalcium phosphate monohydrate (MCPM) and calcium oxide (CaO) in 1M phosphate buffer (pH=7.4) and dicalcium phosphate dihydrate (DCPD) and calcium hydroxide [Ca(OH)₂] in 1 m Na₂HPO₄ solution, respectively, to improve their mechanical strength. The increased compressive strength was caused by phosphorylated chitosan's strong Ca²⁺-binding capacity, which was able to tightly link the newly produced hydroxyapatite (HA) particles together by polymeric chains. The findings showed that P-chitosan-forced calcium phosphate cements offered some favourable properties for medical applications. **(Wang *et al.*,2001)**

The broad spectrum biofilm inhibition and eradication of photocatalytic composites against *Staphylococcus epidermidis*, *Pseudomonas aeruginosa* PAO1, and *Escherichia coli* O157: H7 under visible light irradiation was demonstrated **(Shen *et al.*.,2021)**

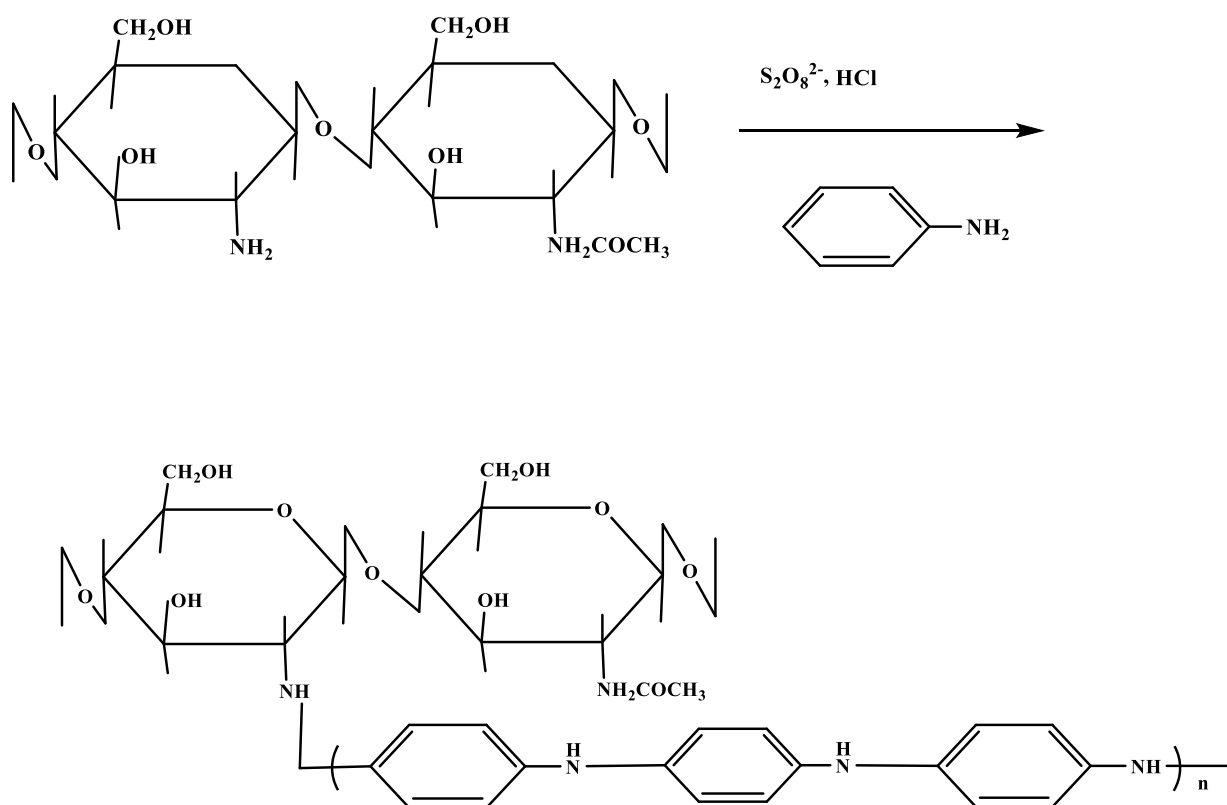
Cell adhesive peptide Gly-Arg-Gly-Asp (GRGD) was photochemically grafted to the surface of chitosan to enhance adherence and growth. The peptide was surface-adsorbed to chitosan and tripolyphosphate anhydrous crosslinked chitosan (chitosan-TPP) surfaces, and then 0.025 m of GRGD-SANPAH (N-Succinimidyl-6-[4'-azido-2'-nitrophenylamino]-hexanoate) solutions were grafted to the surfaces. GRGD was successfully grafted to create chitosan-GRGD surfaces, according to FTIR spectra and electron spectroscopy for chemical analysis (ESCA). Additionally, semi-quantitative HPLC analysis revealed that the grafting efficiencies for 0.025 m of GRGD to chitosan and chitosan-TPP surfaces were approximately 83 percent and 53 percent. After 36 hours of incubation, human umbilical vein ECs developed and attached well to chitosan-GRGD and chitosan-TPP-GRGD surfaces but did not adhere to chitosan and chitosan-TPP surfaces In conclusion, the chitosan-GRGD and chitosan-TPP-GRGD surfaces were made using a photochemical method that could improve EC adhesion and growth for future tissue engineering applications. **(Chung *et al.*,2002)**

Semi-IPN (interpenetrating polymer network) hydrogels made of β-chitosan and PEG diacrylate macromer were created by UV irradiation and their properties were investigated in order to build a polymeric biomedical material. Chitosan was used to crosslink hydrophilic PEG(polyethylene glycol) diacrylate macromer segments. The EWC (equilibrium water content) of all hydrogels was high, ranging from 77 to 83 percent. Due to the reduced re-orientation of the PEG macromer and β-chitosan during crosslinking, the degree of crystallinity of PEG macromer chains in the semi-IPNs significantly decreased. Additionally, in semi-IPNs, the glass transition temperature of PEG macromer segments rose

almost to room temperature. With increasing β -chitosan content, the mechanical strength in the dry state increased. (Lee *et al.*, 1997)

For the regulated release of medications, semi-interpenetrating polymer network (IPN) microspheres of chitosan and polyethylene glycol (PEG) were created. An alternative approach to chemically crosslinking chitosan microspheres containing the model medication isoniazid (INH) is suggested and assessed. FTIR analysis is used to perform a structural examination of the microspheres. Investigations were conducted into the swelling behavior, hydrolytic degradation, structural changes to the microspheres, and loading capacity (LC) of the microspheres for INH. The produced microspheres had a drug loading capacity of 93%, indicating that they are acceptable for controlled pharmaceuticals in an oral sustained delivery system. (Gupta *et al.*, 2001)

Graft copolymers of polyaniline and chitosan have been synthesized. They are soluble in aqueous solution and form self-supporting materials, including thick films and fibers. Upon protonic doping, their conductivities rise from less than $\sim 10^{-7}$ S/cm to the 10^{-2} to 10^{-1} S/cm range, depending on the initial chitosan-to-aniline ratio. Spectroscopic studies show the grafting and demonstrate that the electronic states are similar to those of the emeraldine and photonically doped emeraldine forms of polyaniline. (Yang *et al.*, 1989)

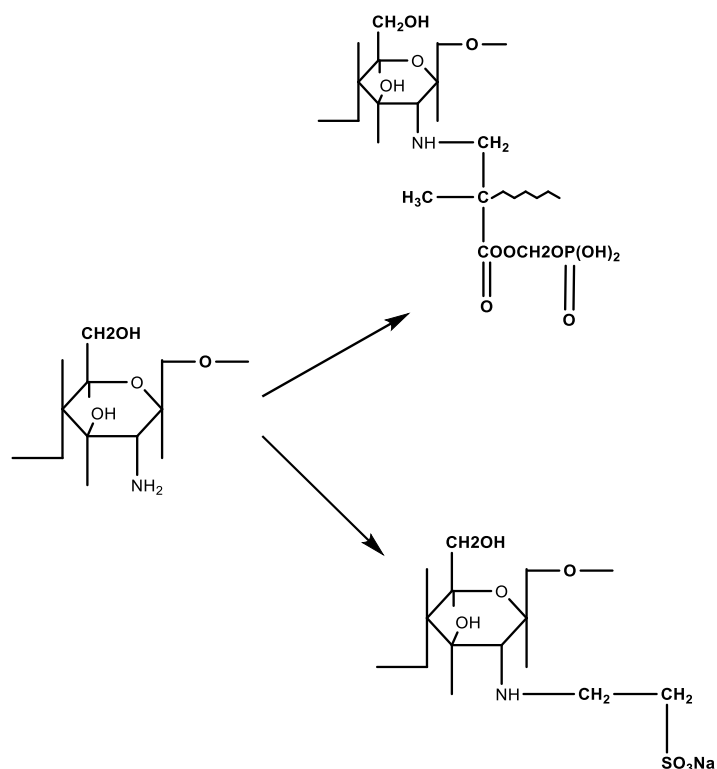


CHITOSAN GRAFTED POLYMER

Graft copolymerization is one of several techniques which is the most alluring since it is a practical way of changing the chemical and physical properties of natural polymers. Reactive groups that can be grafted onto chitosan come in two different varieties. Initially, the free amino groups on deacetylated units and then the hydroxyl groups on the C3 and C6 carbons on acetylated or deacetylated units. By covalently attaching a molecule, the graft, to the chitosan backbone, chitosan can be grafted to produce functional derivatives. Recent studies have also demonstrated that primary deviation followed by graft modification will greatly improve the water solubility and bioactivities of chitosan, such as its antibacterial and antioxidant capabilities. **(Xie *et al.*,2002)**

Chitosan was acylated with maleic anhydride in a formamide medium, producing trisubstituted products (on one amine and two hydroxyl groups of the saccharide unit) was shown by IR spectroscopy, carboxylic group titration, and olefin bond content analysis. Crosslinked polymers have been produced by copolymerizing trisubstituted maleilated chitosan with acrylamide in aqueous solution. With a rise in the proportion of maleilated chitosan in the original reagent combination and a decrease in the dilution of the initial mixture of reaction components, their swelling in water diminishes. In this instance, consumption of maleilated chitosan double bonds ranges from 40 to 70%.**(Berkovich *et al.*,1983)**

The graft reaction into chitosan and the inclusion of MAP mono(2-methacryloyl oxyethyl) acid phosphate(MAP) and VSS vinylsulfonic acid sodium salt (VSS) onto chitosan by FTIR and ¹³C-NMR spectra improved the antibacterial activity. *Candida albicans* could only be killed by a pH of 5.75, and at that pH, chitosan-g-MAP, DA-90, DA-70, and chitosan-g-VSS all had antibacterial activity that was 95, 85, 82, and 75 percent effective, respectively. All of the samples' antibacterial activities—aside from chitosan-g-MAP—were greater than 95% against *Trichophyton rubrum*. For *Trichophyton violaceum*, DA-70 and DA-90 displayed 60–70% antibacterial activities, while chitosan-g-MAP had astounding antimicrobial activity of 95% or more. **(Jung *et al.*, 1999)**



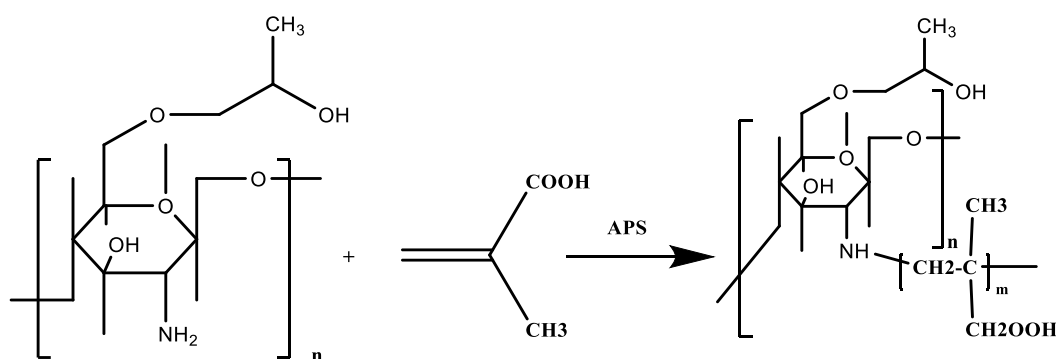
Based on grafted copolymers of Poly (L-lysine) PLL and chitosan made by ring-opening polymerization, **Yu *et al.*,2011** proposed combining the strong cationic property of PLL with the biocompatibility and low toxicity of chitosan to generate an effective non-viral gene delivery method (ROP)

Membrane penetration was significantly aided by the ability of arginine and guanidino moieties to go across cell membranes. The backbone of chitosan was conjugated with arginine in this study to create a brand-new chitosan derivative called arginine modified chitosan (Arg-CS). According to the findings, Arg-CS/DNA complexes were marginally less hazardous than Arg-CS. The luciferase expression mediated by Arg-CS was significantly increased to around 100 times compared with the luciferase expression mediated by chitosan at varied pH conditions, utilising HeLa cells as the target cells and pGL3-control as the reporter gene. These findings indicate that Arg-CS is a good choice as a reliable and effective vector for transfection and gene delivery. (**Zhu *et al.* ,2007**)

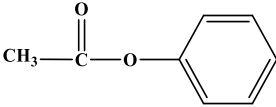
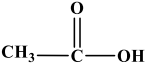
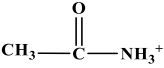
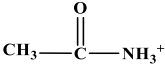
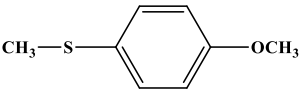
The grafting of L-phenylalanine onto low molecular weight chitosan is accomplished by using carbodiimide as a coupling agent.. The LMW CS-g-Phe and its complex show very reduced toxicity to fibroblast cells. The release of DNA from the complex is very fast in high pH media (tris buffer, pH 8.0 and carbonate buffer, pH 9.5), and relatively slow or more sustainable in neutral and low pH ones (PBS, pH 7.4 and citric acid/trisodium citrate buffer, pH 3.0). The results suggest that the LMW CS-g-Phe be an alternative promising carrier for negatively charged active molecules(**Yokshan *et al.*,2009**)

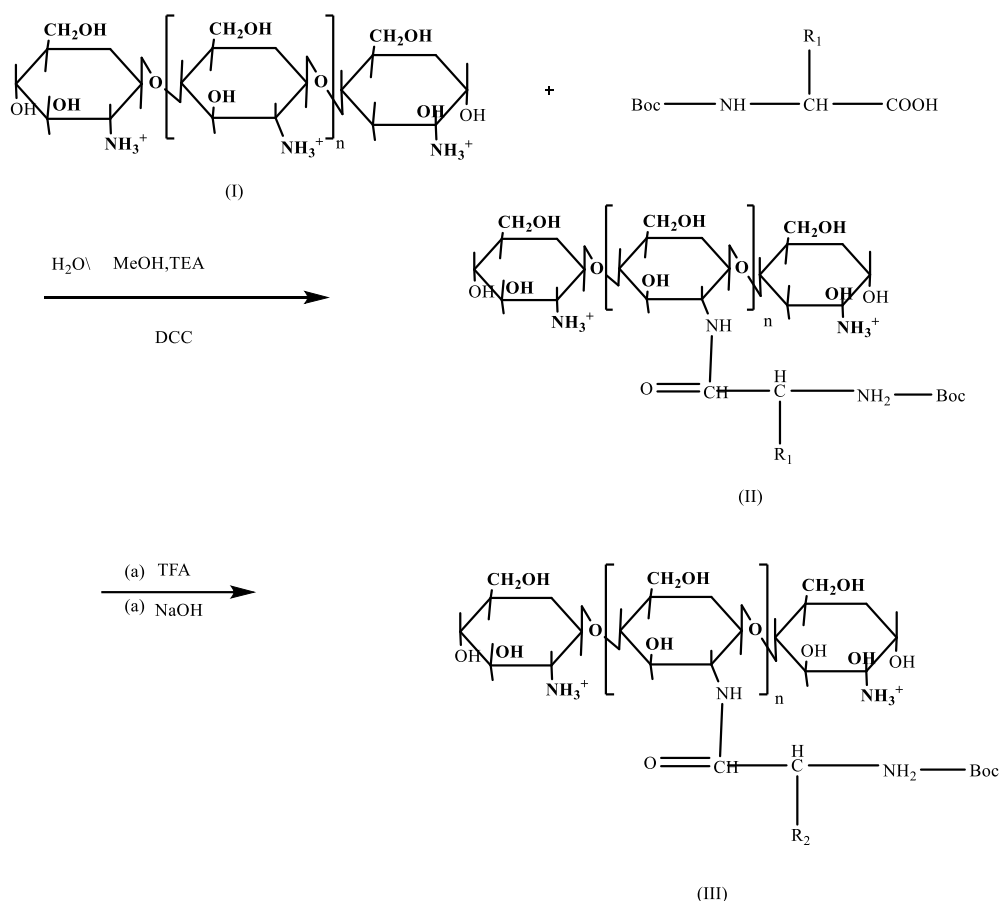
The PLL-grafted chitosan copolymers combine the benefits of chitosan's high biocompatibility with those of PLL's strong pDNA-binding properties. Comprehensive characterization is done of the produced Chi-g-PLL copolymers' chemo-physical characteristics. The in vitro transfection study demonstrates that the copolymers' capacity for gene transfer is significantly greater than that of their starting components, PLL and chitosan. The transfection effectiveness of the copolymers exhibits a positive association with PLL chain length. Our findings indicate that these new Chi-g-PLL copolymers are suitable choices. **(Yu *et al.*, 2011)**

Hydroxypropyl chitosan (HPCTS) was made in order to explore the graft modification of chitosan derivatives. It was then elementally analysed and FTIR described. In an aqueous solution, methylacrylic acid (MAA) was grafted onto HPCTS while utilizing ammonium persulfate (APS) as an initiator. By comparing the FTIR spectra of HPCTS and the Ned copolymer as well as the products' solubility properties, evidence of grafting was discovered. Investigations on the effects of reacting time, temperature, initiator and monomer concentration ratios on grafting % and efficiency **(Xie *et al.*, 2002)**



A chitosan oligosaccharide (COS) derivative by N-conjugation of COS with asparagine(Asn), an amino acid with two amino groups, was synthesised and the antimicrobial effect on *E. coli* growth was compared with other COS derivatives which were N-conjugated with glycine, alanine, aspartic acid, cysteine, and methionine, and unmodified COS. A ¹³C ET-NMR, an FT-IR, an elemental analyzer, and an asparagine N-conjugated chitosan oligosaccharide (Asn-COS) derivative were used to determine the structure of the molecule. Asn-COS substantially boosted the antibacterial activity against *E. coli* growth when compared to the other COS derivatives and COS itself.. This suggests that the two positive charges on AsnCOS and the two negative charges on the carboxyl group on the bacterial cell wall have a strong electrostatic interaction. The results for Asn-COS were as follows: During the course of the three-day culture period, there was no *E. coli* growth, 100% bactericidal activity, 0.002% MIC, and Asn-COS demonstrated potential as a new antibiotic. **(Jeon *et al.*, 2001)**

S.No	Amino acid pf AA-COS	R ₁	R ₂	II → III
1	Glycine	H	H	(a)
2	Alanine	CH ₃	CH ₃	(a)
3	Aspartic acid			(a),(b)
4	Asparagine			(a)
5	Cysteine		CH ₃ —SH	(a),(b)
6	Methionine	CH ₃ CH ₂ —S—CH ₃	CH ₃ CH ₂ —S—CH ₃	(a)



Synthetic scheme of chitosan oligosaccharide derivatives (AA-COS)N-conjugated with different amino acids(Jeon *et al.*,2001)

By using a straightforward dip-coating technique, chitosan/poly (vinyl pyrrolidone) (CHI/PVP) coatings were created to enhance the antibacterial properties of poly (ethylene terephthalate, or PET). By pretreating PET with polyetherimide, polyacrylic acid, and crosslinking in succession, the binding ability of CHI/PVP coatings was improved. AFM and water contact angle measurements showed that the coatings produced a very hydrophilic surface with minimal roughness. *Staphylococcus aureus* (*S. aureus*) and *Escherichia coli* (*E. coli*) adhesions to PET coated with CHI/PVP were greatly diminished. *E. coli* and *S. aureus* were successfully eradicated by CHI/PVP coatings' bactericidal activity, and PVP's addition ostensibly improved the anti-adhesion capability.. Human umbilical vein endothelial cells' cell morphology and activity assessments, as well as in vitro cytotoxicity assays, demonstrated the high biocompatibility of CHI/PVP coatings.(Wang *et al.*,2012)

OBJECTIVE

Graft copolymerization is the most alluring approach since it may be used to change the chemical and physical characteristics of natural polymers. Many studies have also demonstrated the chitosan's water solubility and bioactivities, such as antibacterial and antioxidant capabilities, significant enhancement by graft modification.(*Xie et al.,2002*)

L and D amino acids are employed in a variety of processes, including pharmaceutical manufacturing, enzyme structure and function study, and the development of bactericides. This is because they degrade easily and are non-toxic.(*Hao et al., 2017*)

Glycerol is utilized as a plasticizer and to enhance the biofilm's physicochemical characteristics. Because of its hydrophilic properties, the glycerol molecule can be employed to make biofilms more elastic and wettable.(*pinto et al.,2018*).

By creating intermolecular crosslinking with chitosan hydroxyl groups, polyethylene glycol (PEG) is employed to affect the swelling, solubility, and release properties, according to a report(*Gupta et al .,2001*). Chitosan grafted with HEMA increased thermal stability (*Singh et al.,1998*)

Since application of graft polymerization is greater in the medical field, the present work aims to

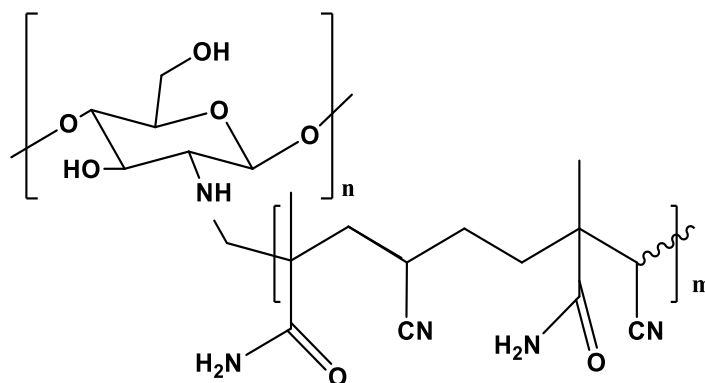
- ✓ Study the graft polymerization of chitosan with various amino acids such as L-threonine,, L-hydroxy proline, and with the combination of both L-threonine and L-hydroxy proline.
- ✓ Prepare sol-gel of acid-grafted chitosan using glycerol. polyethylene glycol and 2-Hydroxy ethyl methacrylate as a binder
- ✓ Coat the prepared polymer on 316 stainless steel using dip coater
- ✓ Characterize the structure of polymers by the FT-IR technique
- ✓ Determine the thermal stability of the polymers by TGA
- ✓ Evaluate the surface and thickness of the steel films by SEM



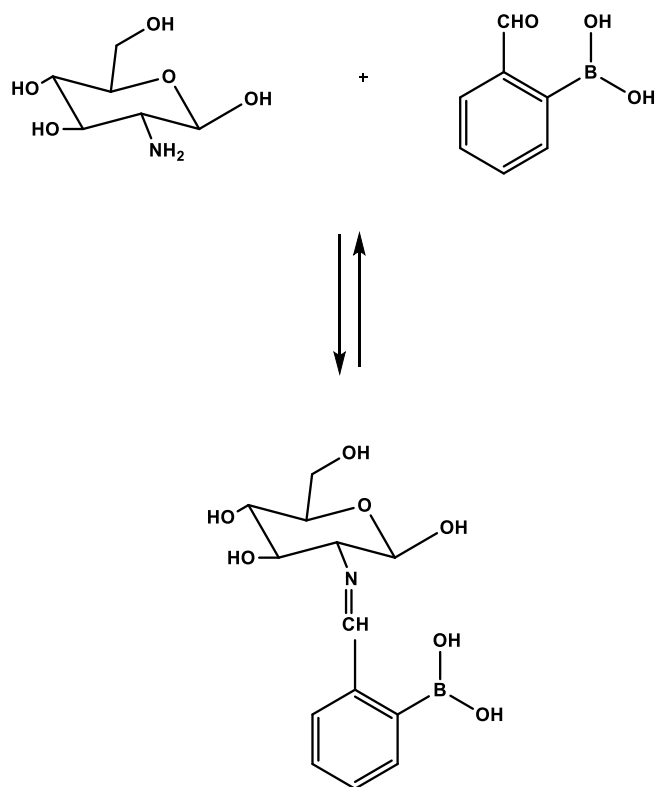
REVIEW OF LITERATURE

2.REVIEW OF LITERATURE

Raorane *et al.*,2022 prepared this work to create chitosan (CS)-modified materials and assessed their capacity to prevent *Candida* biofilm growth. Different polysaccharides have been utilised to suppress biofilm formation by drug-resistant fungi. To further enhance its applicability, CS was grafted with methacrylamide (MA), acrylonitrile (AN), and hyaluronic acid to create the CS-g-poly (MA-co-AN) HA complex. Spectroscopic methods verified grafting and complex creation. CS-g-poly (MA-co-AN) HA showed considerable antibiofilm action at 200 g/ml against *Candida albicans*

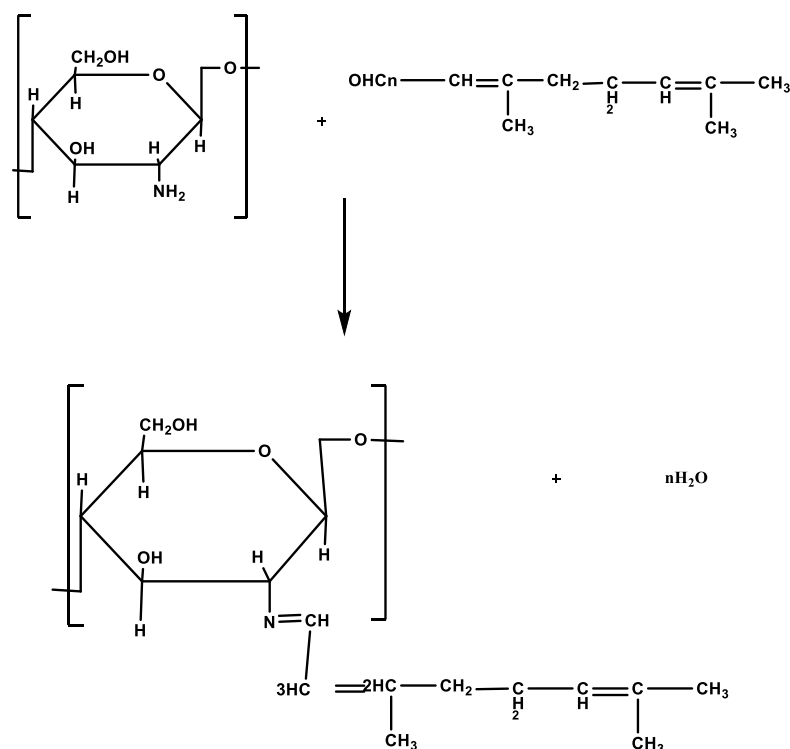


Alincia *et al.*,2016 prepared chitosan -iminoborane network by reacting chitosan with 2-formyl phenyl boronic acid. Supramolecular chitosan hydrogels were generated from low molecular weight molecules with covalent and hydrogen bonds . FTIR and NMR spectroscopy confirmed the formation of dual iminoboronate-chitosan network through chemo-physical crosslinking. The iminoboronate network's three-dimensional nano structuring improved the mechanical characteristics were confirmed by X-ray diffraction, SEM, and rheological analysis. The hydrogels demonstrated potent antifungal action against biofilms and planktonic yeasts belonging to the *Candida genus*, offering promise as a gentle remedy for vulvovaginitis infections that recur often.



Pinto *et al.*, 2018 introduced a method where glycerol was added to the biofilm as an option to increase its wettability and flexibility. In order to characterize this biomaterial's wettability, microstructure, mechanical, and chemical properties, plasticizer was added at low and high concentrations. Glycerol addition to chitosan produced biofilms with more enhanced uniform surfaces without making significant changes to its chemical structure. It also improved flexibility and wettability

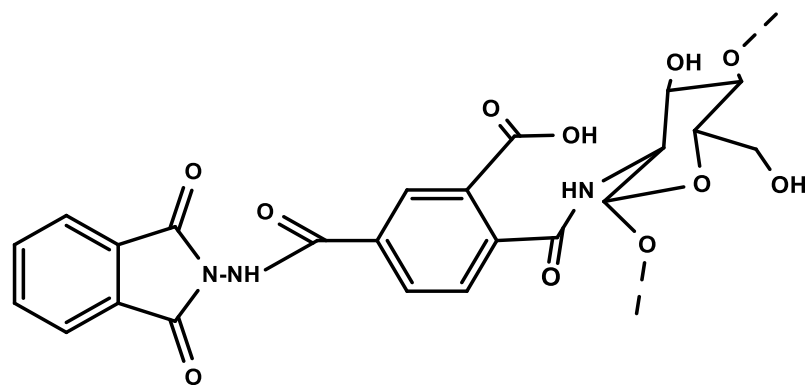
Jin *et al.*, 2009 synthesized the Schiff base using a chitosan and citral reaction that is carried out under high-intensity ultrasound. The antibacterial properties of the substance on *Escherichia coli*, *Staphylococcus aureus*, and *Aspergillus niger* were examined. The results indicate that the Schiff base of chitosan had better antimicrobial activities than chitosan.



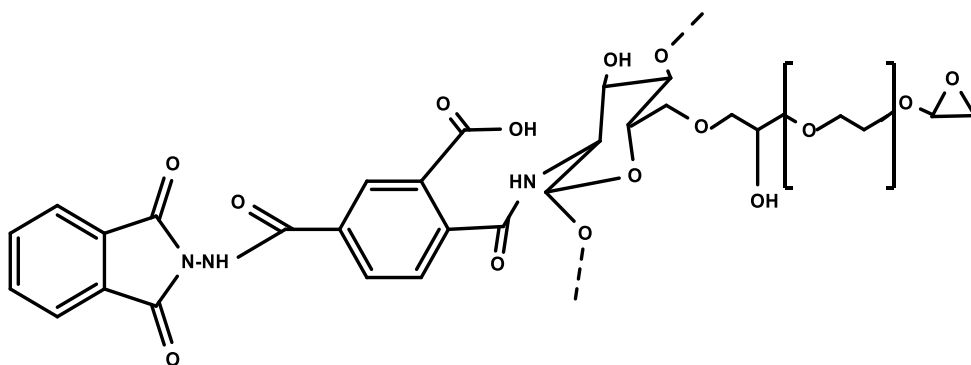
Singh et al., 1998 used 2-hydroxyethyl methacrylate (HEMA) to graft chitosan films utilizing a mCo gamma-irradiation approach. The effect of graft level on the change in physico-chemical characteristics of the chitosan was studied. The study indicated that the increase in graft level decreased the tensile characteristics.. The grafted films displayed increased thermal stability.

Hernandez et al., 2016 created layer-by-layer hyaluronan/chitosan (HA/CHI) nanofilms with enhanced the antibacterial efficacy against *Staphylococcus aureus* and *Pseudomonas aeruginosa*. In this arrangement, chitosan (CHI) exhibited antibacterial properties, whereas HA produced a soft, highly hydrated, and nontoxic coating. The pH values of the biopolymer stem solutions were used as the basis for HA/CHI optimization. The spread plate counting method was used to assess the antibacterial efficacy of HA/CHI nanofilms against both microorganisms. These outcomes were connected to both their chemical and morphological characteristics

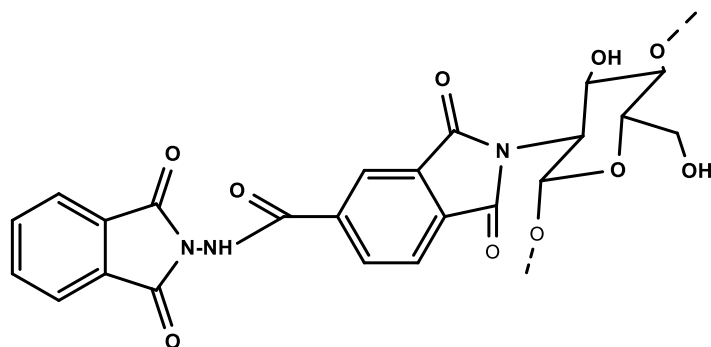
Kandile et al., 2021 introduced the modification of chitosan such amic acid(CS -6)at room temperature, Chitosan with crosslinker (PEGDG) noted as CS-7, imide (CS -8) thermally, and CS-6NPs using TPP with anhydride (5) respectively and was successful in optimizing its properties as an anti-inflammatory, antibacterial, and antitumor. CS-6 and CS-7 displayed higher thermal stability and anti-inflammatory behaviour, while CS-6 NPs showed excellent antibacterial efficiency due to their high surface area.



CS-6



CS-7



CS-8

Umar et al., 2014 employed an ammonium persulfate initiator to graft polystyrene onto the chitosan backbone. The copolymer was used successfully to remove colours from aqueous solutions since the inclusion of polystyrene increased its porosity

Yokoyama et al., 2002 created a novel calcium phosphate cement with α -tricalcium phosphate (α -TCP) and tetracalcium phosphate (TeCP) as the solid components and chitosan, glucose, and citric acid solution as the liquid component powder-based elements. Because of its chewing-gum-like consistency after mixing, this cement could be shaped into the required shape and showed good biocompatibility in both soft and hard tissues. The results of this investigation showed that the concentration of citric acid in the liquid component affects both the mechanical characteristics and biocompatibility of the cement. This study employed liquid components of 20 percent and 45 percent citric acid to evaluate the influence of acid.

Parker et al., 2015 assessed the effects of mixing PEG, at 6,000 or 8,000 g/mol, with chitosan in sponge on *in vitro* vancomycin and amphotericin B elution, eluate activity, and cytocompatibility, as well as on the prevention of a bacterial biofilm *in vivo*. *In vitro*, amphotericin B and vancomycin were both released by blended chitosan sponges. All evaluated amphotericin B eluates continued to be active against *Candida albicans*, and vancomycin eluates from blended sponges continued to be active against *Staphylococcus aureus*. The vitality of fibroblasts was reduced by 62–95% in response to amphotericin B eluates collected after 1 hour from blended sponges, but only by 22–60% in response to eluates obtained after 3 hours. Vancomycin-loaded chitosan/PEG 6000 sponge completely removed bacteria from catheters in a mouse model for preventing the growth of *Staphylococcus aureus* biofilms. Other sponges had lower clearance rates.. These findings suggest that the chitosan/PEG blended sponges may be used as adjunctive therapy to prevent wound infections by delivering localised antifungal and/or antibiotic combinations.

Carlson et al., 2008 tested chitosan coated surface against *Staphylococcus epidermidis*, *Staphylococcus aureus*, *Klebsiella pneumoniae*, *Pseudomonas aeruginosa*, and *Candida albicans* on across a 54-hour trial. The results showed reductions in biofilm viable cell counts ranging from 95% to 99.9997% compared to controls. Chitosan-coated surfaces significantly (more than 5.5 10log units) inhibited *S. epidermidis* surface-associated proliferation when compared to a control surface. Comparatively, *S. epidermidis* surface associated growth was greatly reduced by coatings containing a combination of the antibiotics minocycline and rifampin by 3.9 10log units (99.99 percent), but was not significantly reduced by coatings containing the antiseptic chlorhexidine The effects of chitosan were verified using microscopy Chitosan provided a versatile biocompatible framework for developing coatings to guard against contamination on surfaces..

Tang et al., 2010 examined the antibacterial effects of a new water-soluble chitosan derivative, on *Escherichia coli* and *Pseudomonas fluorescens*, two Gram-negative bacteria. The results indicated a

significant suppression in the growth of the *P. fluorescens* and *E. coli* by the two distinct arginine functionalized(6% and 30%) chitosan. Time-dependent killing efficacy tests revealed that 5000 mg/l of chitosan-arginine with 1%, 6%, and 30% substitutions killed 2.7 logs and 4.5 logs of *P. fluorescens* and 4.8 logs and 4.6 logs of *E. coli* in 4 hours, respectively. Even while the 30 percent substituted chitosan-arginine appeared to be more successful at permeating the cell membranes of both *P. fluorescens* and *E. coli*, the 6 percent substituted chitosan-arginine was more effective at slowing down cell growth at low concentrations. Studies using the fluorescent dyes 1-N-phenyl naphthyl amine (NPN), Nile red (NR), and propidium iodide (PI), as well as field emission scanning electron microscopy (FESEM), suggested that the interaction of chitosan-arginine with the cell membrane, which resulted in an increase in membrane permeability which at least was partially responsible for the substance's antibacterial activity.

Cobrado et al., 2012 used *Staphylococcus epidermidis*, *Staphylococcus aureus*, *Acinetobacter baumannii*, and *Candida albicans* strains to assess the antibacterial and anti-biofilm effects of cerium nitrate, low molecular weight chitosan (LMWC), and hamamelitannin. Polyurethane (PUR)-like catheter segments were used to measure the establishment of biofilms, and a tetrazolium reduction test was used to measure metabolic activity using colorimetry. All of the examined microbial strains were inhibited by cerium nitrate, low molecular weight chitosan (LMWC) except for hamamelitannin.

Miles et al., 2016 reported the preparation of grafted N-acetyl-cysteine (NAC) on chitosan using carbodiimide chemistry. Disulfide cross-linkable chitosan was created, which improved the mechanical properties of chitosan materials without the usage of cytotoxic crosslinkers. Cast films of NAC-Ct conjugates were made with degrees of substitution (DS) ranging from 0% to 20%, and the formation of disulfide bonds was stimulated by raising the pH of the reaction medium to 11. Through monotonic tensile testing on hydrated NAC-Ct films, the tensile strength, breaking strain, elastic moduli, and toughness of disulfide cross-linked polymers were examined. XRD was used to determine crystallinity. The results showed that, compared to unmodified chitosan, NAC inclusion and crosslinking in chitosan created harder polymer films with 4-fold higher tensile strength (10 MPa) and 6-fold better elongation (365 percent). Harder polymer films with a 4-fold higher tensile strength (10 MPa) and a 6-fold better elongation were produced by NAC insertion and crosslinking in chitosan (365 percent).

Aidnik et al., 2021 used a water-based synergistic poly electrolyte-surfactant complex (PESC) made of cationic chitosan (Chi), anionic lysine-based surfactant (77KS), and the amphoteric antibiotic amoxicillin (AMOX), bioactive nanolayers with simultaneous protein-repellent and antimicrobial properties were applied to polydimethylsiloxane-based implants. Both formulations were coated in both dynamic and ambient environments, and the results included irreversible deposition, smooth

morphology, roughness, improved surface coverage, increased hydrophilicity, and an increase in water content. With Chi-77KS/AMOX, *E. coli* and *S. aureus* are reduced by 80% and 67 % respectively. Chi-77KS without AMOX demonstrated a 40 % reduction in both bacteria.

Vishu Kumar et al.,2005 analyzed that at pH 3.5 and 37 °C, papain and pronase optimally depolymerized chitosan to produce LMMC (low molecular mass chitosan) and a Chito-oligomeric-monomeric mixture. Depending on the reaction period (1–5 h), the yield of the latter was 14–16 percent and 14–19 percent, respectively, for papain- and pronase-catalyzed reactions. In comparison to native chitosan, the Chito-oligomeric-monomeric mixture demonstrated superior growth inhibitory action against *Bacillus cereus* and *Escherichia coli*.

Liu et al., 2012 created genipin crosslinked chitosan (GC) with polyethylene glycol (PEG) and zinc oxide (ZnO) nanocomposites, zinc oxide nanoparticles were equally dispersed throughout the GC/PEG matrix. The greater swelling ratios were visible in GC/PEG/ZnO nanocomposites when the pH dropped to an acidic state. ZnO's used in the GC/PEG matrix effectively reduced bacterial growth. As the amount of zinc oxide in the GC/PEG/ZnO nanocomposites increased antibacterial activity also increased. By doping zinc oxide with a modest amount of Ag nanoparticles, the antibacterial activity was enhanced more successfully. Based on both swelling and antibacterial properties, it was concluded that GC/PEG/ZnO/Ag nanocomposites might be used successfully as antibacterial wound-dressing films.

Yu et al.,2019 studied the mechanical properties, microstructures, thermal stability, transparency, WVP, oil permeability, and antibacterial properties of composite films consisting of chitosan (CS) and polylysine (PL) with different CS to PL ratios. The contact angles of the CS/PL mixtures continuously decreased as the weight percentage of PL increased, and the tensile strength of the CS/PL films steadily decreased. Comparable pure PL and CS films have slightly higher thermal stability than CS/PL composite films. The addition of PL enhanced the transparency of the CS/PL films, and they work well as oil and water vapour barriers. Additionally, they showed antibacterial activity against yeast, *Bacillus subtilis*, and *Escherichia coli*. CS/PL films were potential possibilities for food-packaging materials because of their ease of fabrication, good mechanical properties, high transparency, high thermal stability, biocompatibility, and broad antibacterial capabilities.

Hao et al.,2022 effectively produced the Matrine@Chitosan D-Proline (Mat@CS-Pro) nanocapsules with pH-responsive antibacterial performance and biofilm dispersibility. The Mat@CS nanocapsules were first made using the microemulsion technique, and then D-proline was immobilized on their surfaces. The Matrine@Chitosan D-Proline nanocapsules maintained exceptional antibacterial capabilities against *E. coli*, *S. aureus*, and *P. aeruginosa*. Such nanocapsules displayed biofilm prevention characteristics, particularly for gram-negative bacterial strains, after adding D-proline to the Mat@CS surface, with a reduction of up to 74% after 3 days of incubation. The Mat@CS-Pro

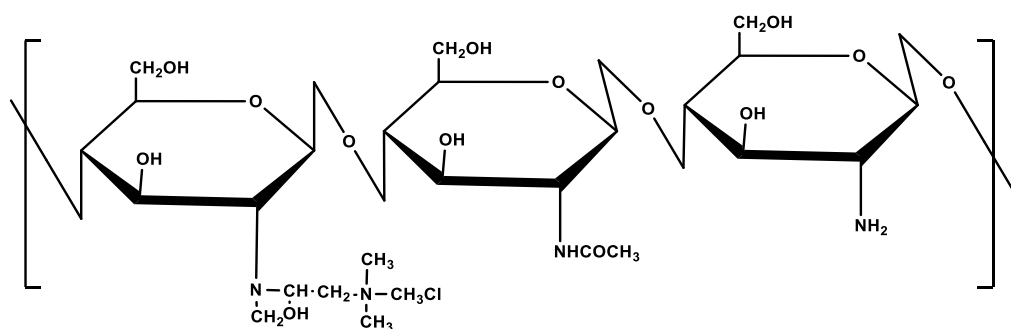
nanocapsules also exhibited extraordinary pH-responsive characteristics, expanding in acidic environments and contracting in alkaline ones. Due to the structural modifications, matrine's releasing behaviours were stronger as the pH of the surrounding environment changed from alkaline to acidic, and it displayed exceptional antibacterial activities in an acidic environment.

Kumar *et al.*, 2007 synthesized low molecular weight chitosans (LMWC) of molecular weight 9.5-8.5 kDa that were obtained by pronase-catalyzed non-specific depolymerization (at pH 3.5, 37 °C) of chitosan than on native chitosan and studied antibacterial activity of *Bacillus cereus* and *Escherichia coli*. Additionally, higher carbohydrate and protein contents as well as cytoplasmic enzymes in the cell-free supernatants were indicative of hole formation and permeabilization of the bacterial cells, which were also indicated by SEM. The proteins that were released were discovered to be cytoplasmic/membrane proteins by N-terminal sequence analysis. When exposed to GLC, *E. coli*'s supernatant displayed fatty acid profiles, supporting the detachment of lipopolysaccharides into the medium, whereas *B. cereus*'s indicated the release of surface lipids.

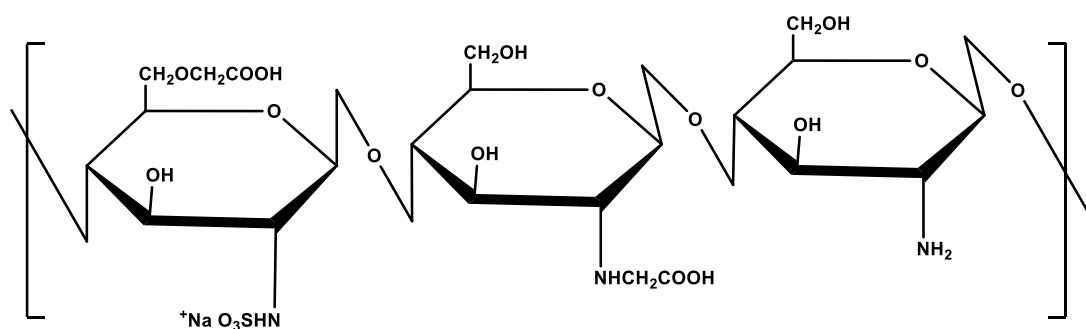
Huang *et al.*, 2001 demonstrated Poly(L-lysine)-g-poly(ethylene glycol) (PLL-g-PEG) to chemisorb on anionic surfaces, including different metal oxide surfaces, offering a high level of resistance to protein adsorption. Through the use of angle-dependent X-ray photoelectron spectroscopy (XPS), time-of-flight secondary ion mass spectrometry (RAIRS), and reflection-absorption infrared spectrometry (RAIRS), the analytical and structural characteristics of PLL-g-PEG adlayers on niobium oxide (Nb₂O₅), tantalum oxide (Ta₂O₅), and titanium oxide (TiO₂) surfaces were examined (ToF-SIMS). The PLL backbone was thought to be situated directly at and parallel to the oxide/polymer interface, while the PEG chains are more frequently oriented in the direction perpendicular to the surface. PEG-related secondary ion fragments with strong decreased metal (oxide) intensities dominate both

Bulwan *et al.* , 2012 experienced a straightforward LbL approach to creating ultrathin multilayer films made of chitosan derivatives under realistic biological circumstances. Microscopic examinations (SEM, AFM), as well as the MTT viability test, and other research, showed that the coatings also protected surfaces from the growth of bacterial (*Staphylococcus aureus*) biofilm. The antiadhesive and anticoagulant qualities of such chitosan films had been demonstrated in studies using human plasma and fresh blood, making them promising as protective coverings for medical devices and things that come into contact with blood. Numerous biomedical applications may be found for these adaptable protective ultrathin coatings, which were based on charged derivatives of the widely used polysaccharide chitosan.

Cationic derivative of chitosan



Anionic derivative of chitosan



Wang *et al.*,2020 created a unique approach for the manufacture of chitosan(CS) copolymers containing tryptophan (Trp) or phenylalanine (Phe). The findings demonstrated that CS could be easily grafted with Trp and Phe, with grafting rates of 4.7% and 6.8%, respectively. In addition to altering the symmetry and backbone structure of CS, the grafting significantly reduced its heat stability and viscosity. According to rheological investigations, grafting tryptophan (Trp) or phenylalanine (Phe) onto Chitosan caused it to exhibit characteristics of an elastic material. Additionally, research revealed the strong biocompatibility and antioxidant activity of Trp-CS and Phe-CS. The nrecent research created a practical method for creating CS nano-conjugates that could be investigated as potential biomaterials for the food industry.



MATERIAS AND METHODS

3.MATERIALS AND METHODS

- ✓ Low molecular weight chitosan (extra pure) was purchased from Loba chemicals
- ✓ 1% acetic acid is prepared by adding 0.1 ml of concentrated acetic acid to 0.9 ml of water.
- ✓ 0.1 M Ammonium persulphate solution prepared by dissolving 0.2281g of ammonium persulphate in 10 ml of water
- ✓ 316 L stainless steel is cut into 1mm×1mm dimension and 60mm×20mm dimension plates with 0.5 mm thickness.
- ✓ 120 gsm Grit sheet is used to polish 316L stainless steel.
- ✓ The Fourier transform infrared (FTIR) spectrum was recorded by ATR technique in a SHIMADZU PRESTIGE 20 FT-IR Spectrometer. Absorption frequencies were quoted in reciprocal centimeters.
- ✓ The Thermal gravimetric analysis was done by STA module with no reference from 30°C to 500° C.
- ✓ The Scanning Electron Microscope was performed using ZEISS sem analyzer with 1000 magnification.

PREPARATION OF ACID-GRAFTED CHITOSAN

Preparation of L-threonine grafted chitosan

0.2509 g of low molecular weight chitosan was dissolved in 3 ml of 1% acetic acid (solution A) 0.0258 g of L-threonine was dissolved in 6 ml of 0.1 M ammonium per sulphate (solution B). Solution B was added to solution and the mixture was stirred for 24 hours. After formation of polymer, the contents were treated with acetone. The solid obtained was filtered and dried. 0.2643g yield was obtained

Preparation of L-Hydroxy proline grafted chitosan

0.2509 g of low molecular weight chitosan was dissolved in 3 ml of 1% acetic acid (solution A) 0.0258 g of L-Hydroxy proline was dissolved in 6 ml of 0.1 M ammonium per sulfate (solution B). Solution B was added to the solution and the mixture was stirred for 24 hours. After the formation of polymer, the contents were treated with acetone. The solid obtained was filtered and dried. 0.2708 g yield was obtained

Preparation of THRLHP-g-CS grafted chitosan

0.2509 g of low molecular weight chitosan was dissolved in 3 ml of 1% acetic acid (solution A) 0.0129 g of L-Hydroxy proline and 0.0129 g of L-threonine was dissolved in 6 ml of 0.1 M ammonium per sulphate (solution B). Solution B was added to the solution and the mixture was stirred for 24 hours. After the formation of the polymer, the contents were treated with acetone. The solid obtained was filtered and dried. 0.2716 g yield was obtained

Coating of acid-grafted chitosan polymer on 316L stainless steel:

0.1g of acid-grafted chitosan (THR-g-CS, LHP-g-CS, and THRLHP-g-CS) was dispersed in 30 ml of 1% aqueous acetic acid solution using ultrasonication till it was homogenized. 0.1g of glycerol, polyethylene glycol, and HEMA was added and stirred for six hours. 316 L stainless steel samples were cut into 10mm× 10mm dimensions. The samples were polished from 120 grit silicon carbide paper and washed with distilled water followed by ethanol and kept in acetone for 15 minutes. The prepared homogenous solutions are used for dip coating the steel. The dip coating procedure was carried out with different pH by maintaining the pH using NaOH and HCl



RESULTS AND DISCUSSION

4.RESULTS AND DISCUSSIONS

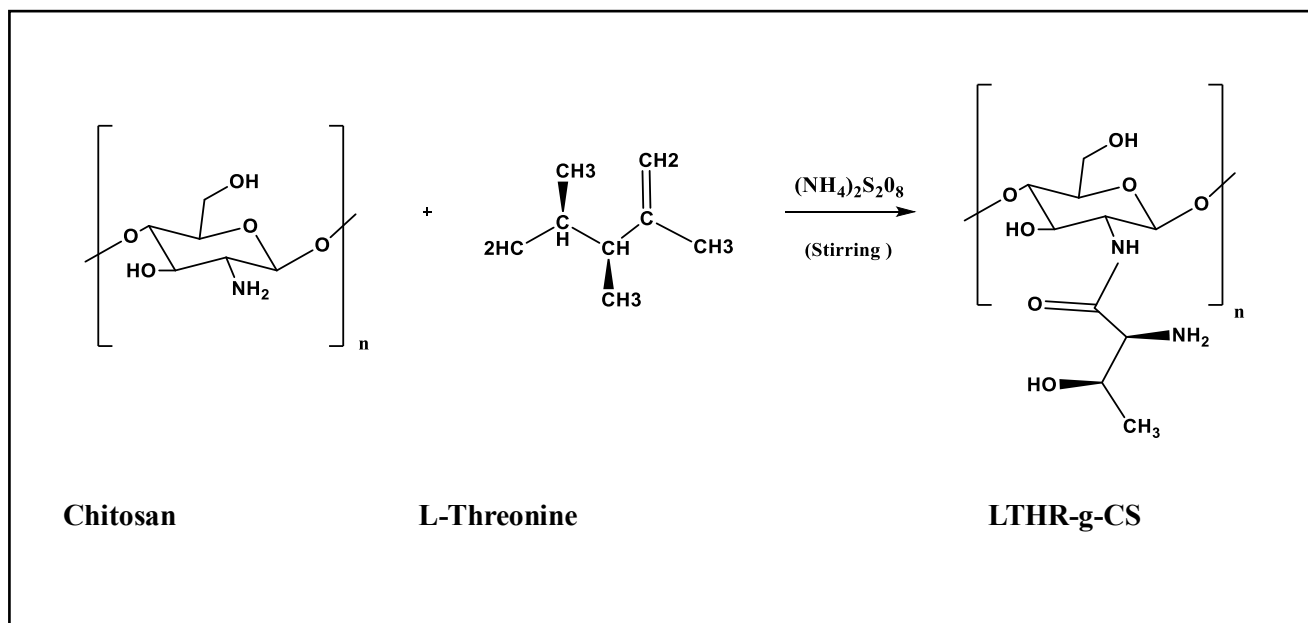
4.1 PREPARATION OF GRAFTED CHITOSAN

The grafting of amino acid with chitosan has been reported by few authors with the different types of products such as phenylalanine and tryptophan grafted chitosan (**Wang *et al.*,2020**) and Poly(L-lysine) grafted chitosan (**Bulwan *et al.*,2012**)

In the present work ,L-threonine, L- hydroxy proline and both L-threonine and L- hydroxy proline was treated with chitosan to obtain highly grafted chitosan polymer. Further, the polymers are coated on 316L stainless steel. The 316L stainless steel was used in dental procedures and implants in the human body (**Gotman *et al.*,1997**)

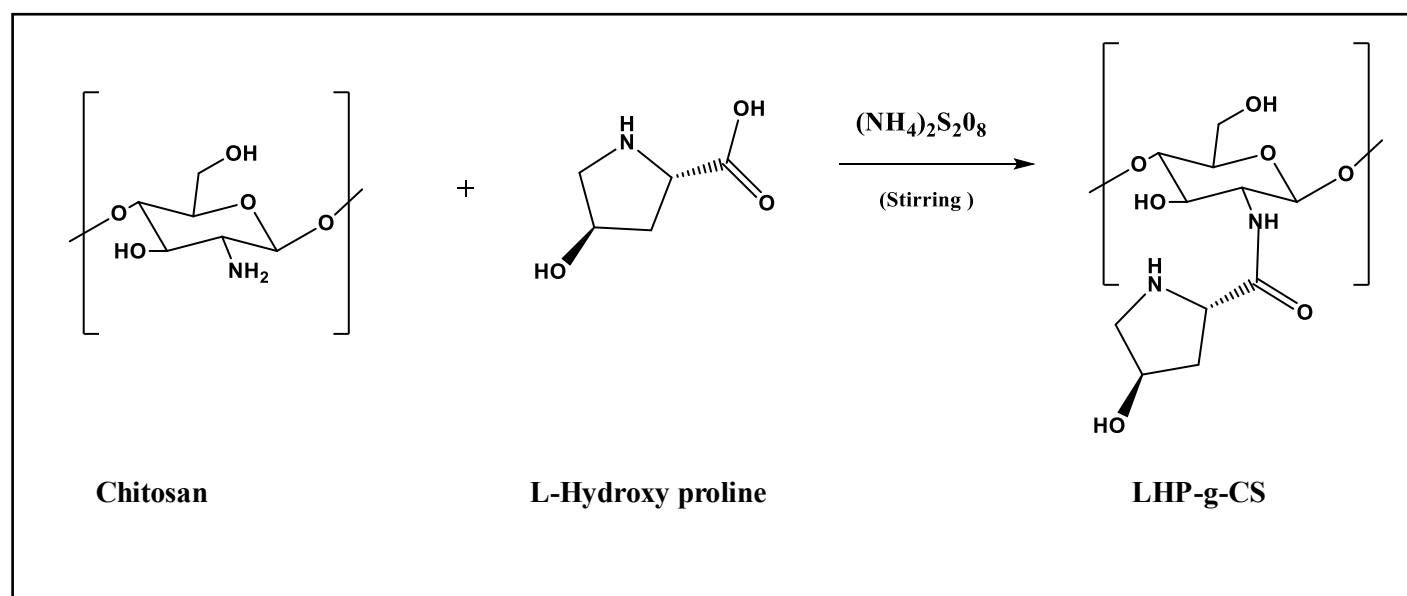
The reaction was carried out by stirring the mixture of acid with 0.1 M ammonium persulphate solution and chitosan with 1% acetic acid for 24 hours, without heat. After the formation of the polymer, the contents were treated with acetone. The solid obtained was filtered and dried. The yield of the products were given in **Table – I**. The sol-gels of the products were made by dissolving the products in 1% acetic acid using ultrasonication and stirred with glycerol, Polyethylene glycol, and Hydroxy ethyl methacrylate for 6 hours. Previously, cured 316L stainless steel was coated with prepared sol-gels

SCHEME I



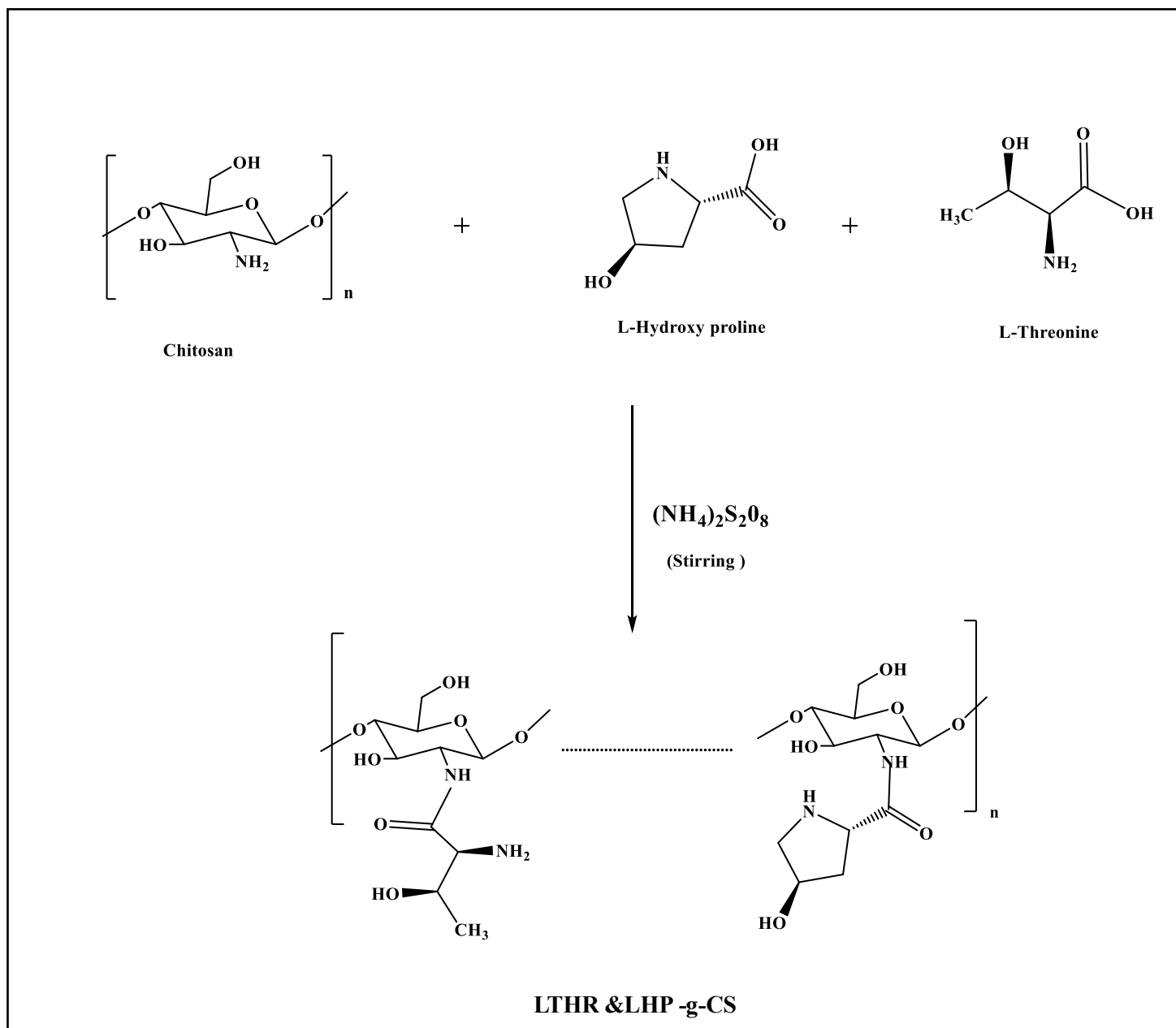
LTHR-g-CS = L-Threonine grafted chitosan

SCHEME II



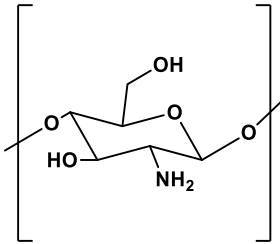
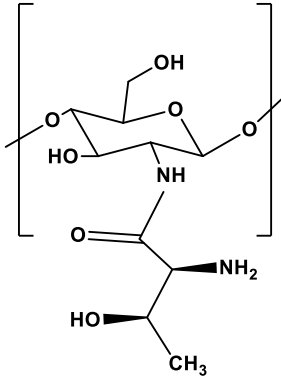
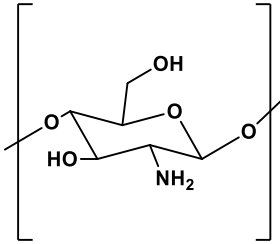
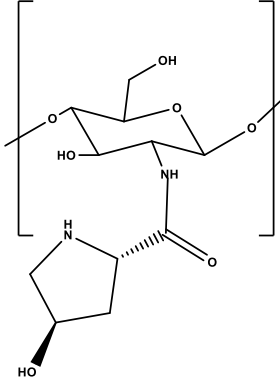
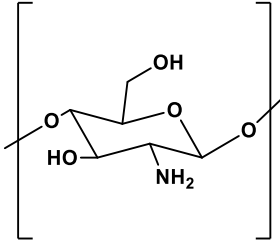
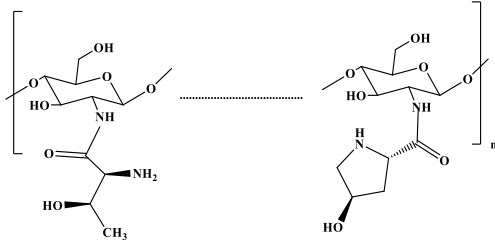
LHP-g-CS = L-Hydroxy proline grafted chitosan

SCHEME III



LTHR & LHP -g-CS = L-Threonine & L-Hydroxy proline grafted chitosan

Table I: The yields of Product Formed

REACTANT	PRODUCT	CATALYST	YIELD
		(NH ₄) ₂ S ₂ O ₈	95.5%
		(NH ₄) ₂ S ₂ O ₈	97.7%
		(NH ₄) ₂ S ₂ O ₈	98.1%

4.2 CHARACTERISATION OF THE SYNTHESISED COMPOUNDS

The synthesized polymers are characterized using FTIR, thermal stability was determined by TGA, solubility test and the surface morphologies of the coated 316L stainless steel was analyzed using SEM analysis

4.2.1 FT-IR ANALYSIS

The IR spectrum of LTHR-g-CS, LHP-g-CS and LTHRLHP-g-CS are shown in **Figure 1**, **Figure 2** and **Figure 3** respectively.

4.2.1.1 L-Threonine grafted chitosan

The FT-IR spectrum of L-Threonine grafted chitosan (**Figure 1**) showed a sharp band in 3451 cm^{-1} corresponded to -OH stretching in chitosan. A peak at 2929 cm^{-1} corresponded to the aliphatic C-H stretching. The stretching vibration of NH-C=O was observed at 1639 cm^{-1} (amide I). A peak at 1414 cm^{-1} indicated C-H bending. A peak 1119 cm^{-1} denoted C-NH stretching vibration of the amide group

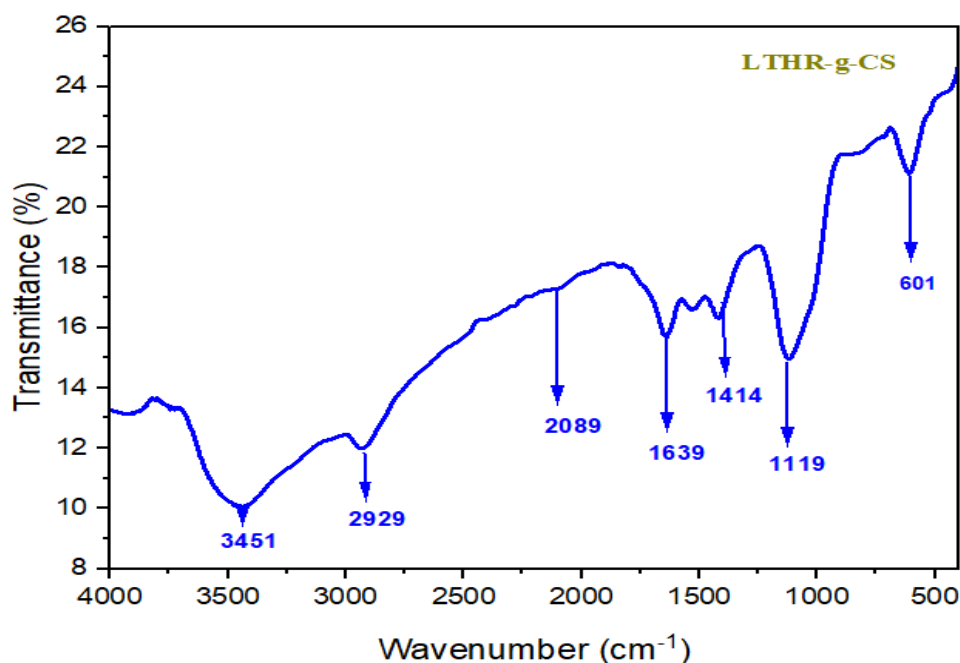


FIGURE 1: FT-IR spectrum of L-Threonine grafted chitosan

4.2.1.2 L-Hydroxy proline grafted chitosan

The FT-IR spectrum of L-hydroxy proline grafted chitosan (**Figure 2**) showed a broad band in 3438 cm^{-1} represented -OH stretching. A peak at 2920 cm^{-1} corresponded to the aliphatic C-H stretching. Peak at 2272 cm^{-1} portrayed the C=C stretching. The stretching vibration of NH-C=O was observed at 1630 cm^{-1} (amide I). A peak at 1414 cm^{-1} indicated C-H bending of alkane. A peak at 1132 cm^{-1} denoted C-NH stretching vibration of the amide group

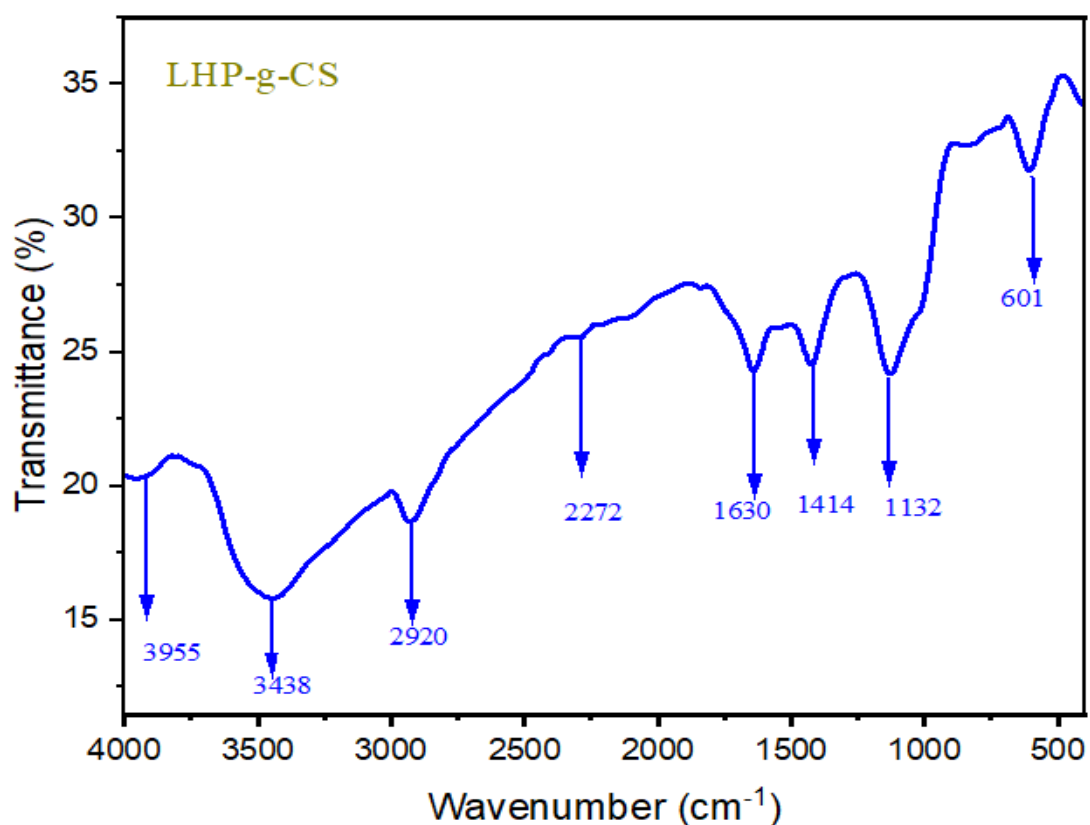


FIGURE 2: FT-IR spectrum of L-Hydroxy proline grafted chitosan

4.2.1.3 L-Threonine &L-Hydroxy proline grafted chitosan

The FT-IR spectrum of LHPLTHR grafted chitosan (**Figure 3**) shows that the compound have a broad band in 3451 cm^{-1} represented -OH stretching .A peak at 2914 cm^{-1} corresponded to the C-H symmetric stretching. Peak at 2488 potrayed the C=C stretching The stretching vibration of NH-C=O was observed at 1650 cm^{-1} (amide I). A peak at 1113 cm^{-1} denoted C-NH stretching vibration of the amide group

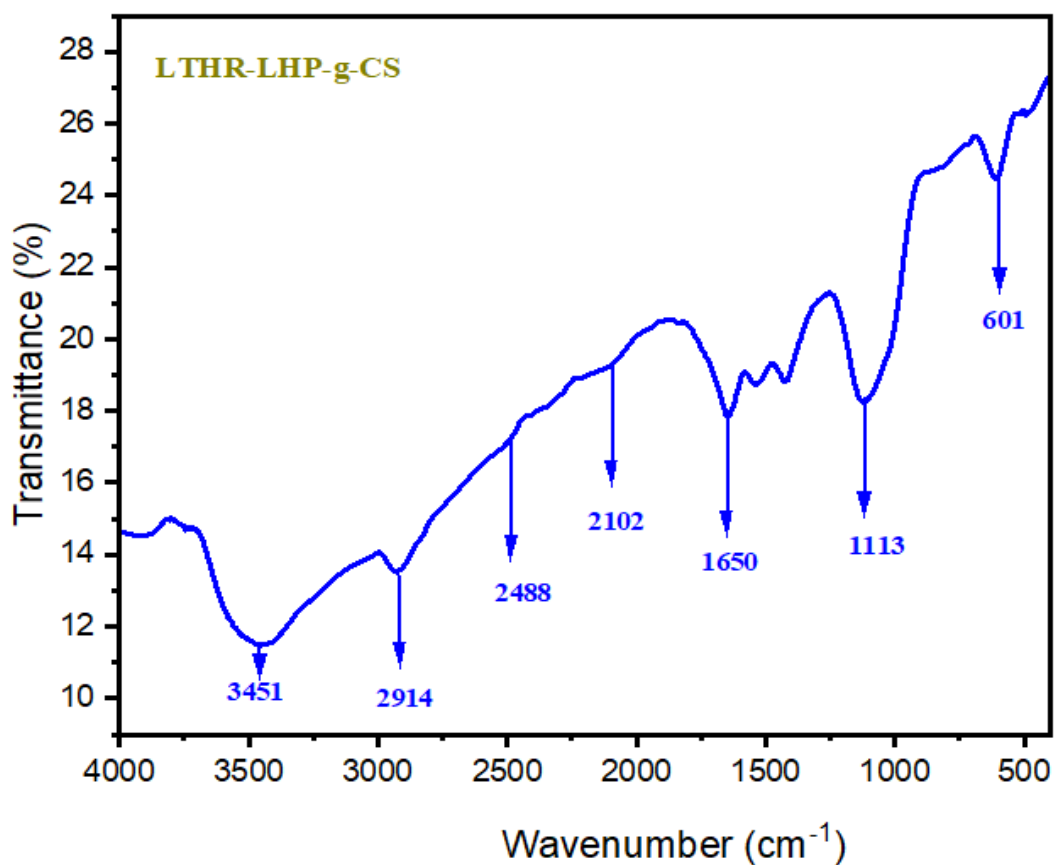


FIGURE 3: FT-IR spectrum of L-Threonine &L-Hydroxy proline grafted chitosan

4.3 TGA and DTA ANALYSIS .

4.3.1 L-Threonine grafted chitosan

The TGA curve of L-THR -g-CS is shown in **Figure 5**. The first weight loss step was observed in the temperature range of 100°C corresponding to the loss of moisture (around 10%). In the temperature range of 150–350°C, non-oxidative thermal degradation of chitosan was found, indicating deacetylation of chitosan and the vaporisation and removal of volatile product. The weight loss percentage was found to be **57.12%**

The first exothermic transition caused by the evaporation of capillary bounded water was detected at the temperature of 43 °C and terminated substantially faster at 62 °C, according to the DTA graph in **Figure 4**. The first endothermic transition, which started at 235 °C and ended at 270 °C, was observed after the thermal phase ended at 230 °C. The third breakdown stage of TG was represented by the second exothermic peak, which was observed between 279 °C and 419 °C.

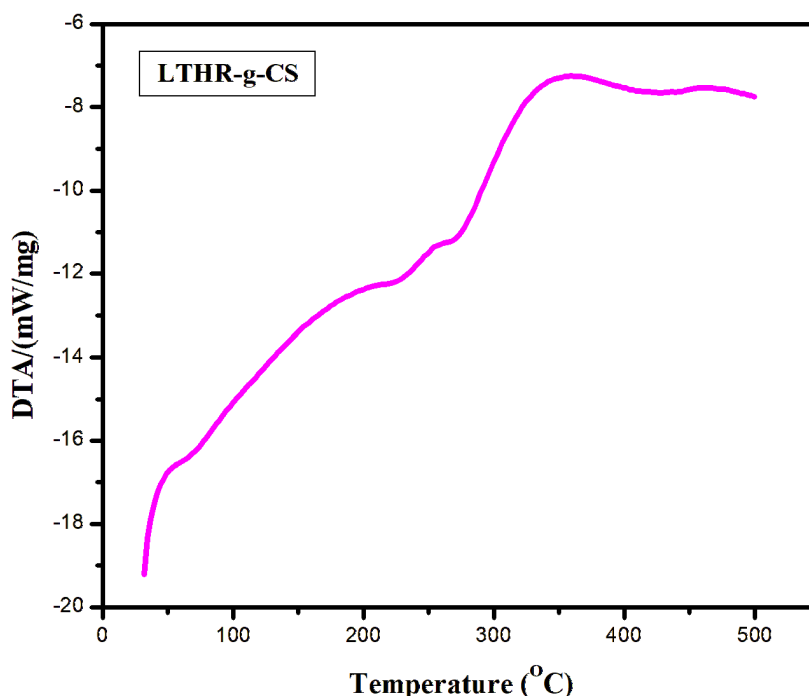


FIGURE 4 : DTA of L- Threonine grafted chitosan

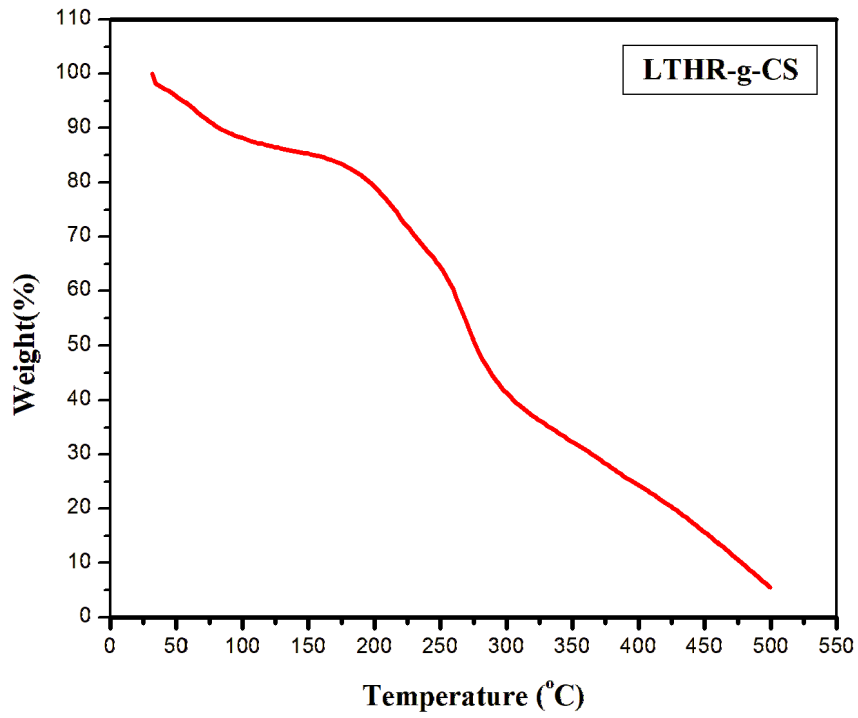


FIGURE 5 : TGA of L- Threonine grafted chitosan

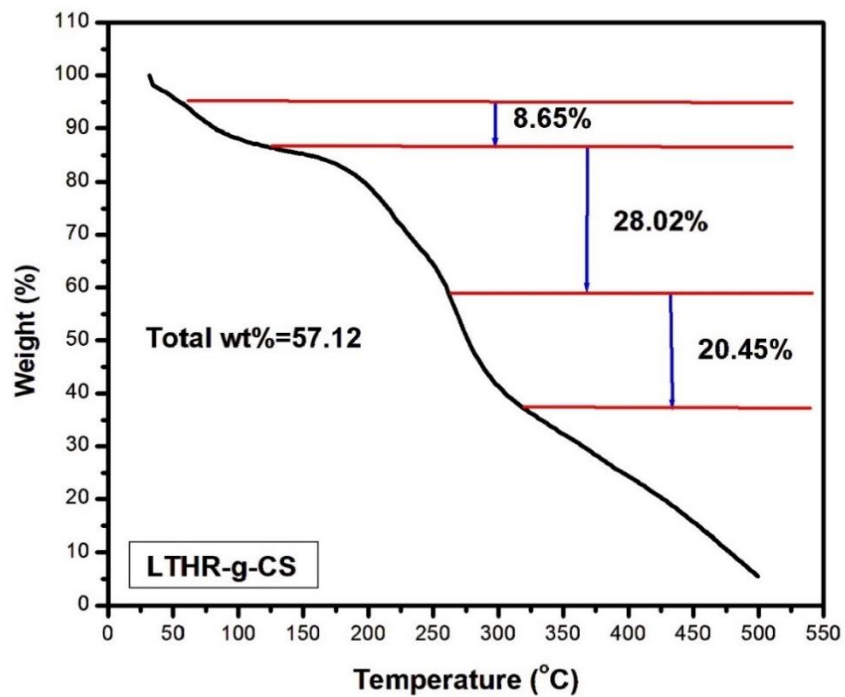


FIGURE 6: Weight loss graph of L- Threonine grafted chitosan

4.3.2 L-Hydroxy proline grafted chitosan

The TGA curve of LHP-g-CS is shown in the **Figure 7**. The depression in the temperature range of 180°C corresponded to the loss of water. As the temperature increased from 175°C to 360 °C, the TGA curve indicated weight loss of 52.6% due to the dehydration of saccharide ring. The total weight loss percentage was 57.12 %

The first exothermic transition caused by the evaporation of capillary bounded water was detected at the temperature of 42 °C and concluded noticeably quicker at 58 °C, according to the DTA graph in **Figure 6**. The first endothermic transition, which started at 235 °C and ended at 268 °C, was observed after the thermal phase ended at 230 °C. The third breakdown stage of TG was represented by the second exothermic peak, which was observed between 281 °C and 431 °C.

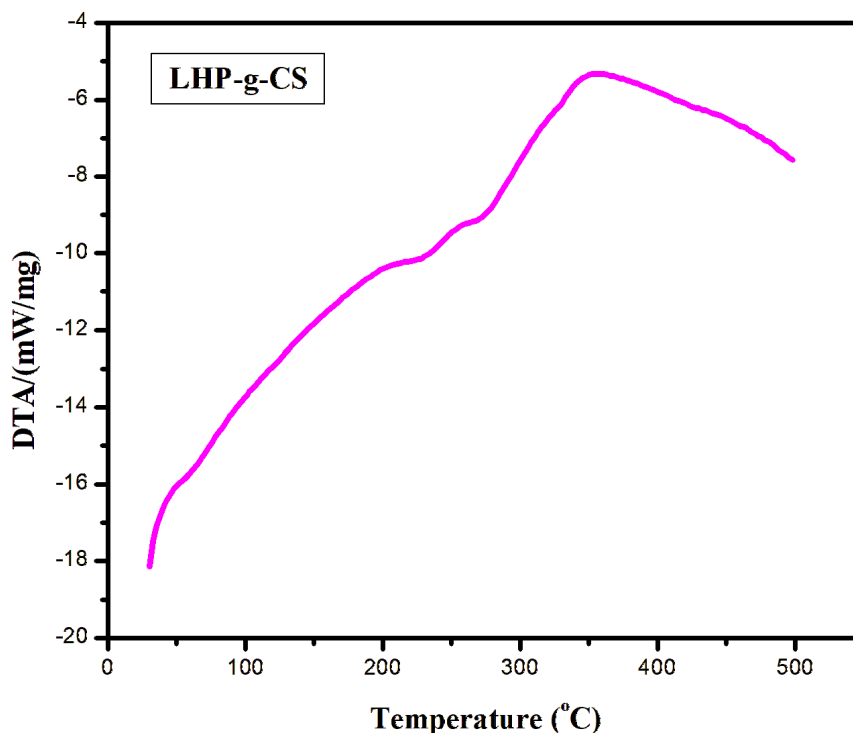


FIGURE 7: DTA of L-Hydroxy proline grafted chitosan

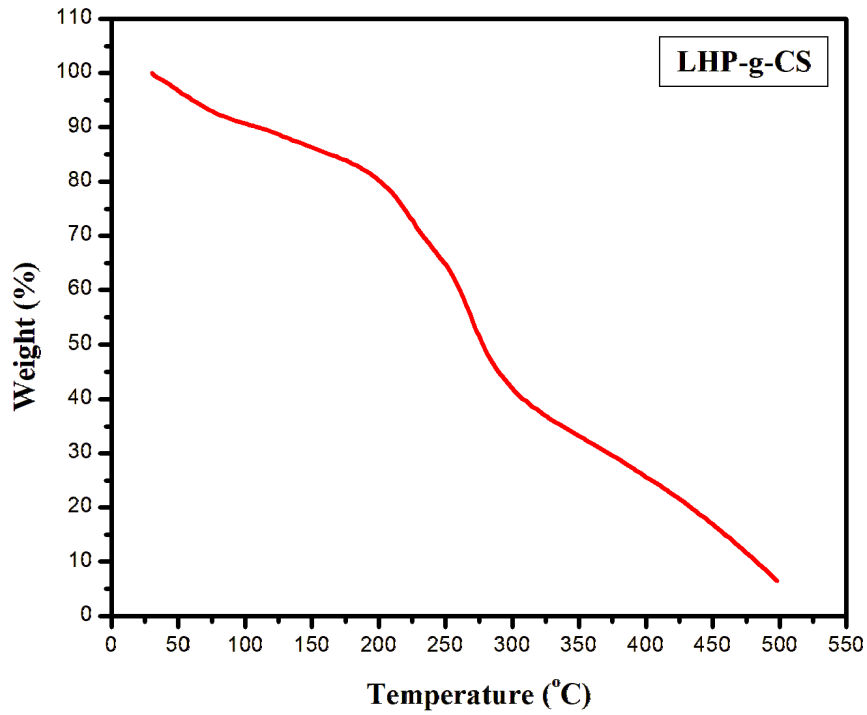


FIGURE 8: TGA of L-Hydroxy proline grafted chitosan

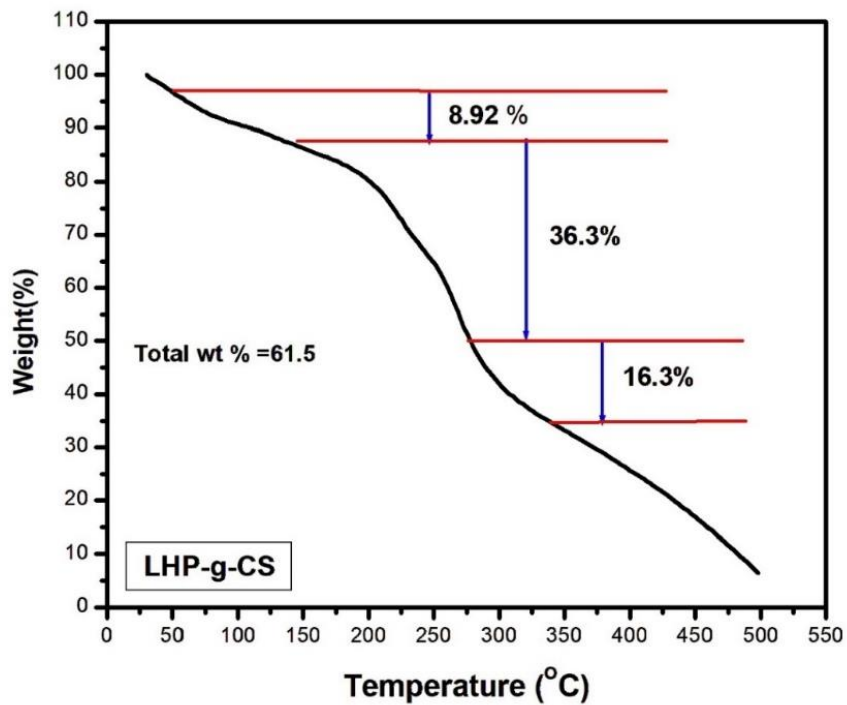


FIGURE 9: Weight loss graph of L-Hydroxy proline grafted chitosan

4.3.3 L-Threonine & L-Hydroxy proline grafted chitosan

The TGA curve of LTHR-LHP-g-CS is shown in the **Figure 9**. The depression in the temperature range of 150°C corresponded to the loss of water. As the temperature increased from 180°C to 360 °C, the TGA curve indicated weight loss of 41.4% due to the dehydration of saccharide ring. The total weight loss percentage was 51.79 %

The first exothermic transition caused by the evaporation of capillary bounded water was detected at the temperature of 37 °C and terminated substantially faster at 53 °C, according to the DTA graph in **Figure 8**. The first endothermic transition, which started at 231 °C and ended at 264 °C, was observed after the thermal phase ended at 230 °C. The third breakdown stage of TG was represented by the second exothermic peak, which was observed between 271 °C and 427 °C.

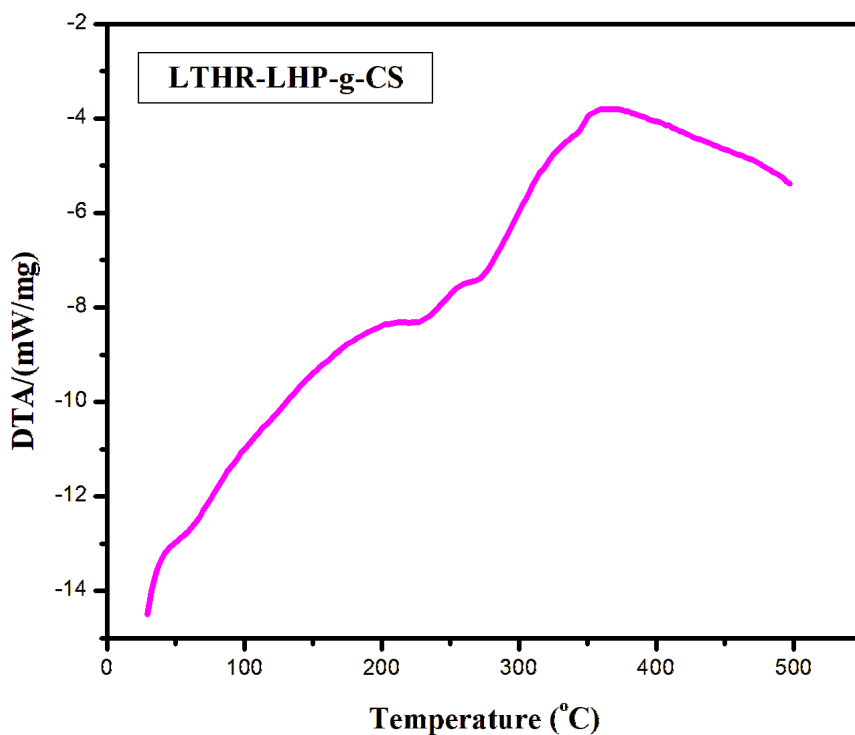


FIGURE 10: DTA of Threonine and Hydroxy proline grafted chitosan

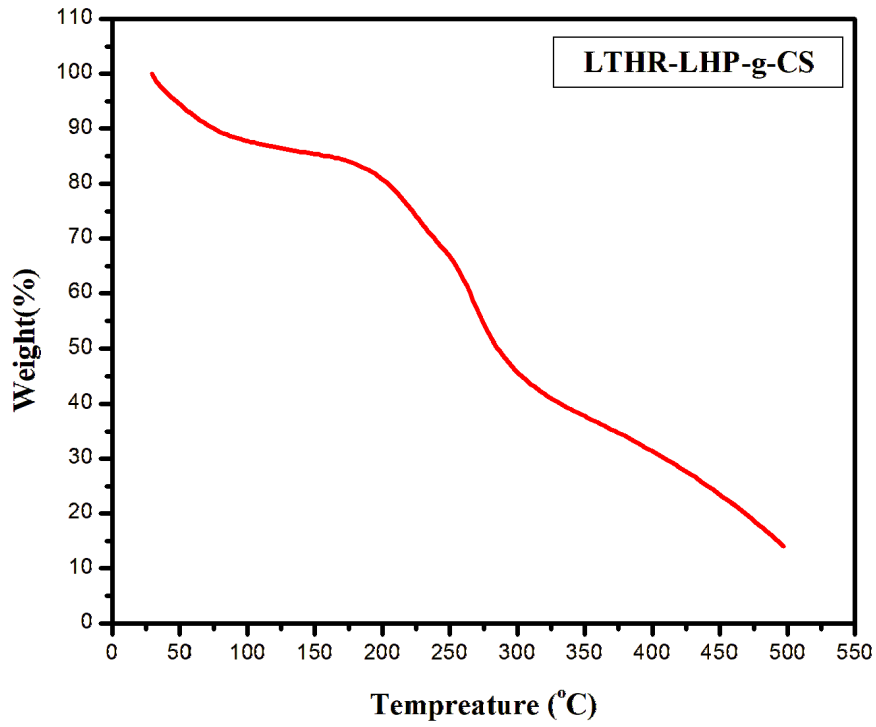


FIGURE 11: TGA of Threonine and Hydroxy proline grafted chitosan

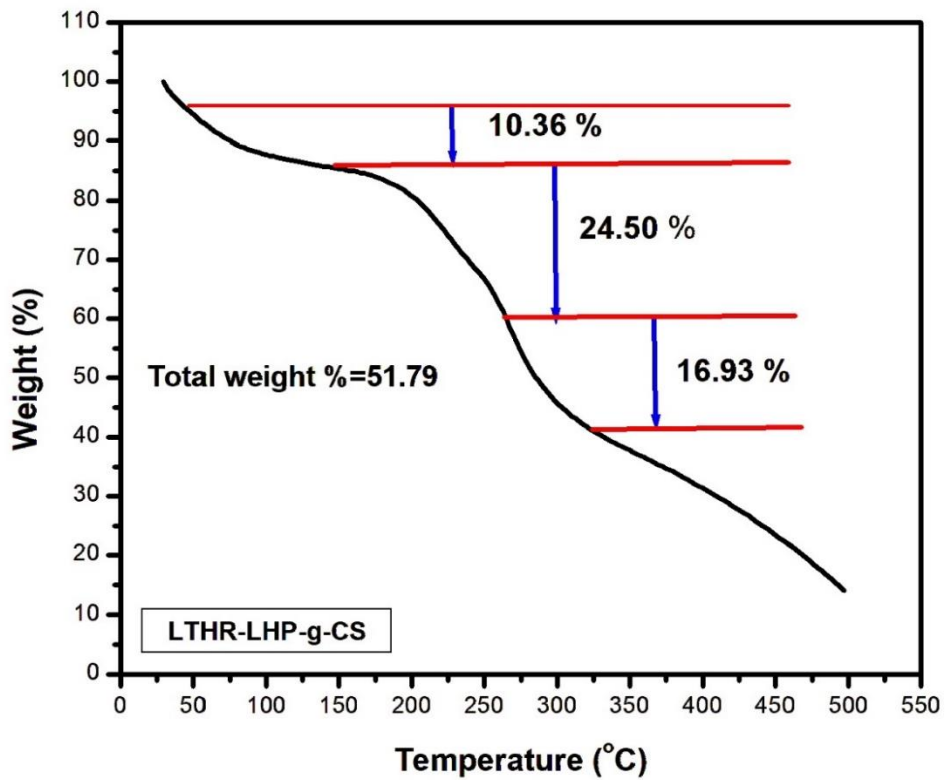


FIGURE 12 :Weight loss graph of Threonine and Hydroxy proline grafted chitosan

4.3.4 The degradation point of LTHR -g-CS shows weight loss at the range 57.1 % , LHP-g-CS at 61.5 and LTHRLHP-g-CS at 51.79% In comparison, two amino acids grafted chitosan shows lesser weight loss percentage than amino acid grafted individually . The results showed that the thermal stability of conjugates LTHRLHP-g-CS was better than LTHR -g-CS and LHP-g-CS. The polysaccharide structure would be disturbed by the hydrophobic alteration of CS amino acids, and the hydrogen bonding contacts of the CS chain would be reduced. The thermal stability of amino acid-grafted chitosan might be explained by some modifications to the chiral structure of the glucose chain and the symmetry and backbone structure of CS. (Wang *et al.*, 2020)

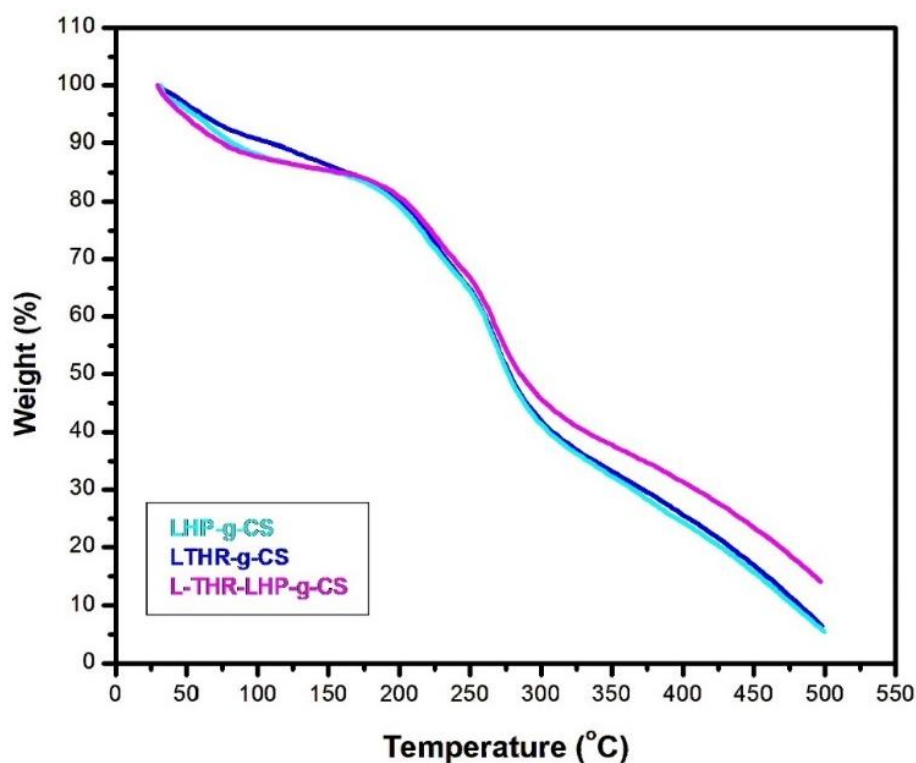


FIGURE 13: TGA curve of amino acid grafted chitosan

4.3.5 The thermal decomposition causes endothermic peaks and oxidative decomposition causes exothermic. The endothermic and exothermic transition was detected at the temperature from 0 °C to 500 °C for LTHR -g-CS, LHP-g-CS, and LTHRLHP-g-CS (**Fig. 11**). Three phase transition was obtained in DTA where two exothermic and one endothermic peaks. It indicated that both oxidative and thermal decomposition has occurred

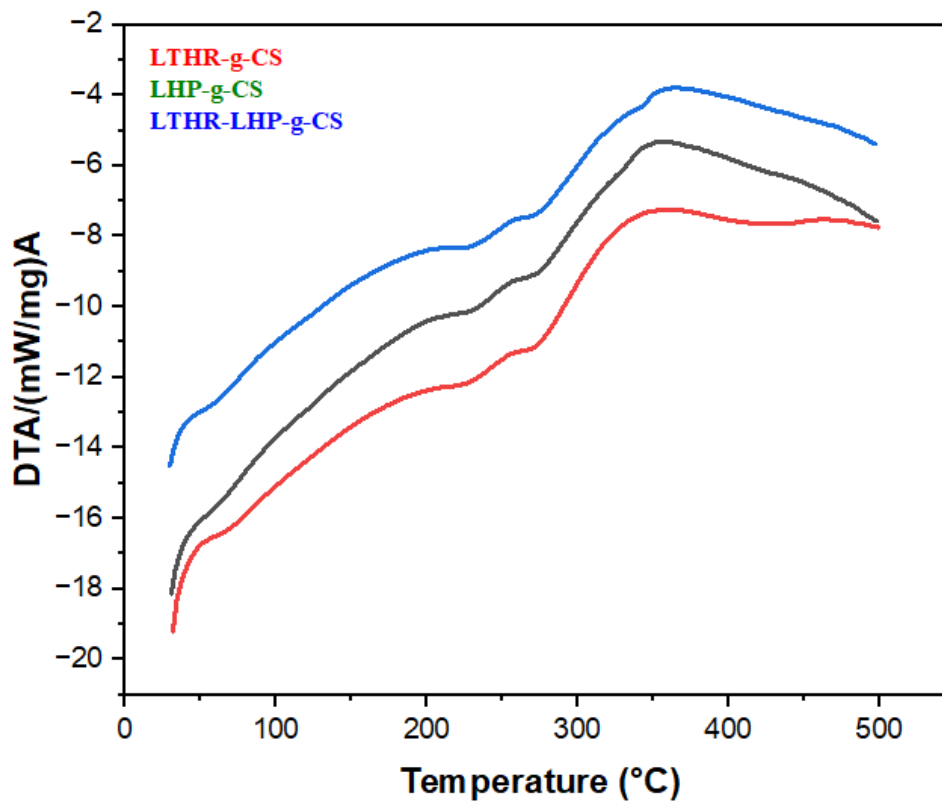


FIGURE 14 :DTA curve of amino acid grafted chitosan

4.4 SEM ANALYSIS

- ✓ The surface features of 316L stainless steel sample without coating and with coating was analysed in ZEISS SEM analyser and the micrographs are shown in **(Figure 13-19)**
- ✓ The SEM image of plain stainless steel (blank) shown in **Figure 13**. The image showed no cracks and coating, only the surface of the steel was observed
- ✓ The SEM images **(Figures 14 to 17)** confirmed that 316L stainless steel is well coated with amino acid grafted chitosan solgels with different binders
- ✓ The difference in surface coating with pH variant is shown in the **Figure 18 and 19**
- ✓ The coating of Chitosan grafted amino acids on 316L stainless steel using polyethylene glycol **(Gupta et al.,2001)** as a binder showed stable coating **(Figure 13,14,15)** which is better than chitosan grafted coating on steel using glycerol **(Pinto et al.,2018)** **(Figure 16)** and HEMA **(Singh et al.,1998)** **(Figure 17)** respectively.
- ✓ Analysis of SEM images revealed that chitosan grafted with amino acids using polyethylene glycol as a binder showed a different coating surface at variant pH whereas grafted chitosan using PEG at pH 6.1 **(Figure 18)** showed better coating than grafted chitosan using PEG a pH 3.4**(Figure 19)**

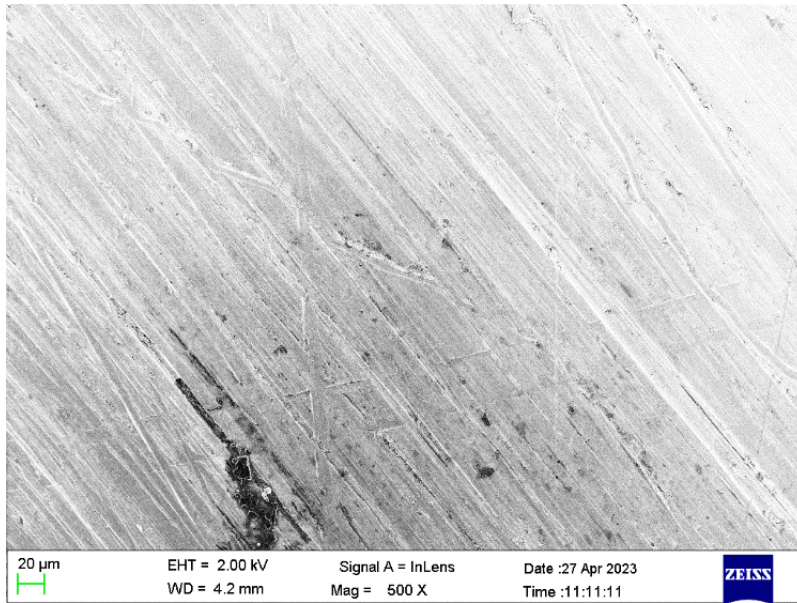


FIGURE 15: SEM image of 316L stainless steel without coating

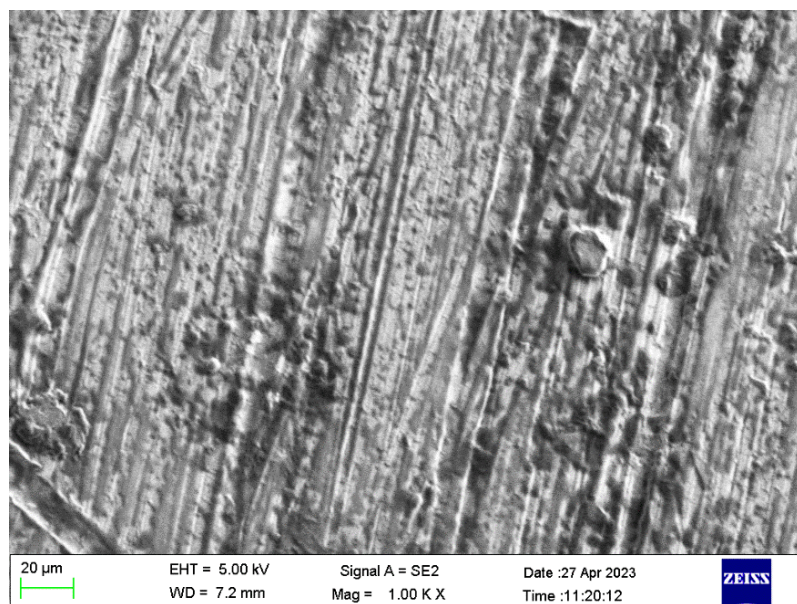


FIGURE 16: SEM image of 316L stainless steel coated with L-THR-g-CS using poly ethylene glycol

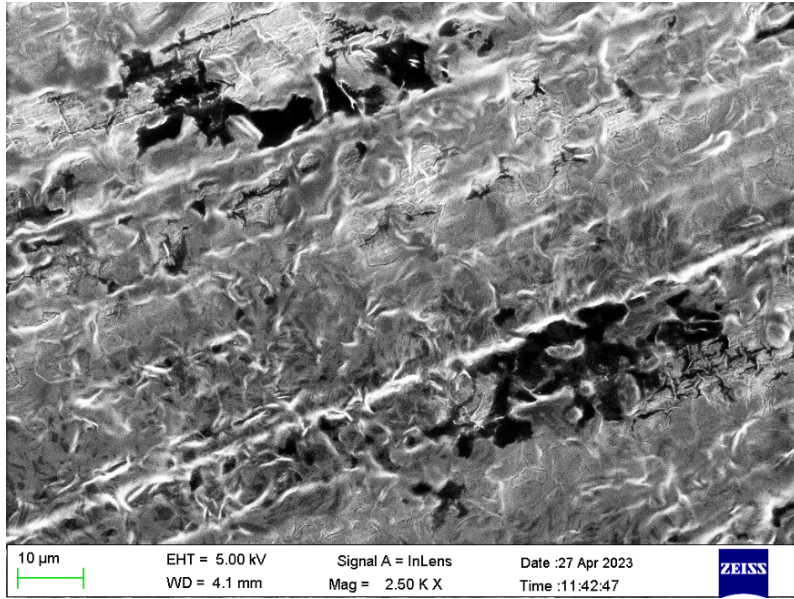


FIGURE 17 :SEM images of 316L stainless steel coated with LHP-g-CS using poly ethylene glycol

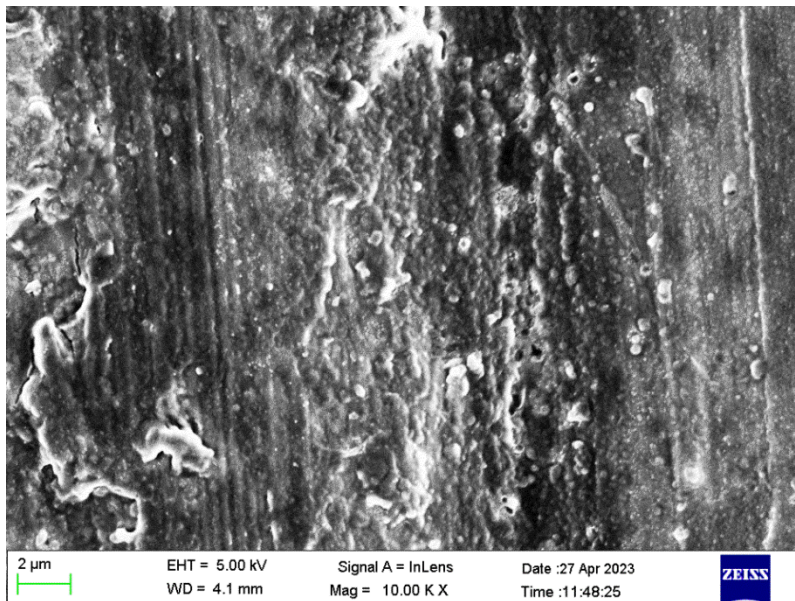


FIGURE 18:SEM images of 316L stainless steel coated with LTHRLHP-g-CS using poly ethylene glycol

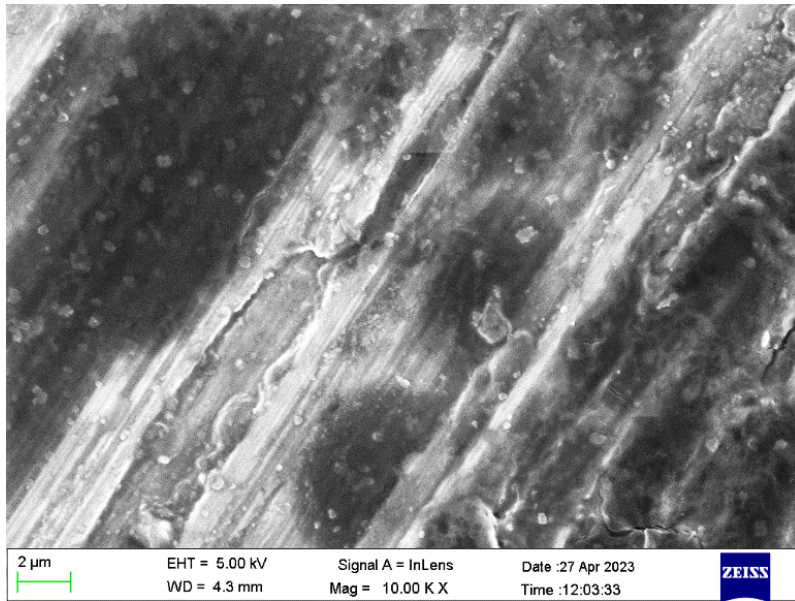


FIGURE 19:SEM images of 316L stainless steel coated with L-THR-g-CS using glycerol

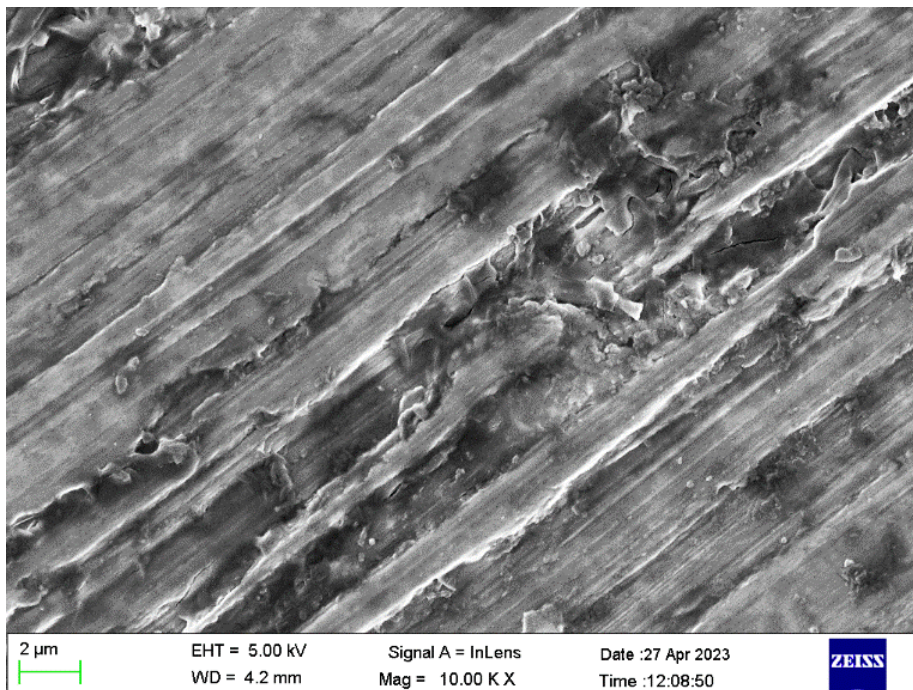


FIGURE 20 :SEM images of 316L stainless steel coated with L-THR-g-CS using Poly-2-hydroxyethyl methacrylate

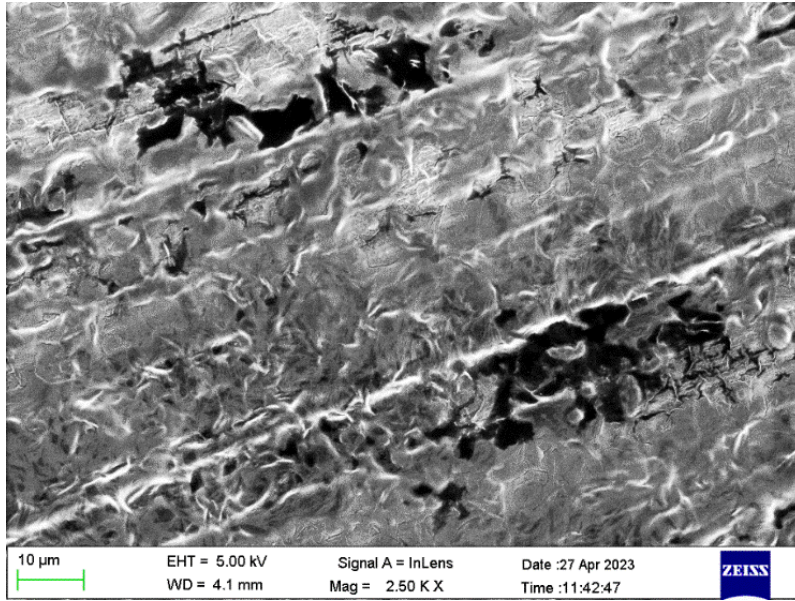


FIGURE 21 : SEM images of 316L stainless steel coated with LHP-g-CS using poly ethylene glycol at PH =6.1

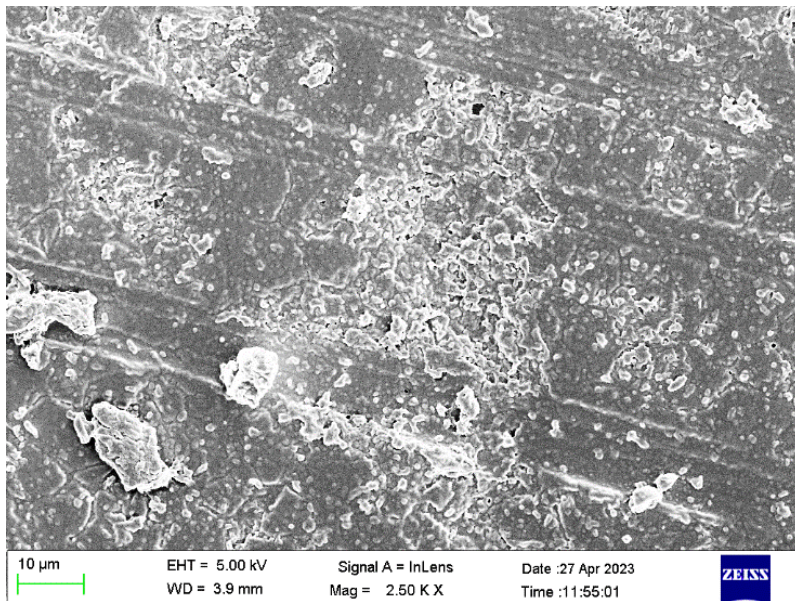


FIGURE 22 : SEM images of 316L stainless steel steel coated with LHP-g-CS using poly ethylene glycol at PH=3.4



SUMMARY & CONCLUSION

5.SUMMARY AND CONCLUSION

The results of the coating of acid grafted chitosan polymeric film in different condition are summarized below,

- ✓ The amino acid grafted chitosan is prepared and synthesised successfully using ammonium per sulphate
- ✓ The prepared compounds were made into sol-gels with different binders such as glycerol, polyethylene glycol (PEG) and hydroxy ethyl methacrylate (HEMA)
- ✓ The prepared gels were coated on a 316L stainless steel by dip coating method
- ✓ The structure of the synthesized polymers was confirmed by FT-IR
- ✓ The thermal stability of the prepared polymers was confirmed by TGA analysis where LTHR-LHP-g-CS showed lesser weight loss when compared to LTHR-g-CS and LHP-g-CS
- ✓ Surface analysis of coated steel was carried out using SEM with different binders and in comparison, PEG shows better binding than glycerol and HEMA
- ✓ The coated steel surface was also verified with different pH variants (3 and 6) to analyse the uniform coating on the steel and pH 6 shows better coating than pH 3
- ✓ In the future, the films can be analysed for antimicrobial, and antibacterial studies so that they can be used as implants for medical applications



6. REFERENCES

- ✓ Kumar, D., Gihar, S., Shrivash, M. K., Kumar, P., & Kundu, P. P. (2020). A review on the synthesis of graft copolymers of chitosan and their potential applications. *International Journal of Biological Macromolecules*, 163, 2097-2112.
- ✓ Mohammed, M. A., Syeda, J. T., Wasan, K. M., & Wasan, E. K. (2017). An overview of chitosan nanoparticles and its application in non-parenteral drug delivery. *Pharmaceutics*, 9(4), 53.
- ✓ Jiménez-Gómez, C. P., & Cecilia, J. A. (2020). Chitosan: a natural biopolymer with a wide and varied range of applications. *Molecules*, 25(17), 3981.
- ✓ Kaur, S., & Dhillon, G. S. (2014). The versatile biopolymer chitosan: potential sources, evaluation of extraction methods and applications. *Critical reviews in Microbiology*, 40(2), 155-175.
- ✓ Islam, S., Bhuiyan, M. R., & Islam, M. N. (2017). Chitin and chitosan: structure, properties and applications in biomedical engineering. *Journal of Polymers and the Environment*, 25, 854-866.
- ✓ Khor, E., & Lim, L. Y. (2003). Implantable applications of chitin and chitosan. *Biomaterials*, 24(13), 2339-2349.
- ✓ Wang, X., Ma, J., Wang, Y., & He, B. (2001). Structural characterization of phosphorylated chitosan and their applications as effective additives of calcium phosphate cements. *Biomaterials*, 22(16), 2247-2255.
- ✓ Shen, H., Durkin, D. P., Aiello, A., Diba, T., Lafleur, J., Zara, J. M., ... & Shuai, D. (2021). Photocatalytic graphitic carbon nitride-chitosan composites for pathogenic biofilm control under visible light irradiation. *Journal of Hazardous Materials*, 408, 124890.
- ✓ Chung, T. W., Lu, Y. F., Wang, S. S., Lin, Y. S., & Chu, S. H. (2002). Growth of human endothelial cells on photochemically grafted Gly-Arg-Gly-Asp (GRGD) chitosans. *Biomaterials*, 23(24), 4803-4809.
- ✓ Lee, Y. M., Kim, S. S., & Kim, S. H. (1997). Synthesis and properties of poly (ethylene glycol) macromer/[beta]-chitosan hydrogels. *Journal of Materials Science: Materials in Medicine*, 8(9), 537.
- ✓ Gupta, K. C., Majeti, N., & Kumar, V. R. (2001). pH dependent hydrolysis and drug release behavior of chitosan/poly (ethylene glycol) polymer network microspheres. *Journal of Materials Science: Materials in Medicine*, 12(9), 753.

- ✓ Yang, S., Tirmizi, S. A., Burns, A., Barney, A. A., & Risen Jr, W. M. (1989). Chitiline materials: soluble chitosan-polyaniline copolymers and their conductive doped forms. *Synthetic Metals*, 32(2), 191-200.
- ✓ Xie, W., Xu, P., Liu, Q., & Xue, J. (2002). Graft-copolymerization of methylacrylic acid onto hydroxypropyl chitosan. *Polymer Bulletin*, 49, 47-54.
- ✓ Berkovich, L. A., Tsyurupa, M. P., & Davankov, V. A. (1983). The synthesis of crosslinked copolymers of maleilated chitosan and acrylamide. *Journal of Polymer Science: Polymer Chemistry Edition*, 21(5), 1281-1287.
- ✓ Jung, B. O., Kim, C. H., Choi, K. S., Lee, Y. M., & Kim, J. J. (1999). Preparation of amphiphilic chitosan and their antimicrobial activities. *Journal of Applied Polymer Science*, 72(13), 1713-1719.
- ✓ Yu, H., Deng, C., Tian, H., Lu, T., Chen, X., & Jing, X. (2011). Chemo-Physical and Biological Evaluation of Poly (L-lysine)-Grafted Chitosan Copolymers Used for Highly Efficient Gene Delivery. *Macromolecular bioscience*, 11(3), 352-361.
- ✓ Zhu, D., Zhang, H., Bai, J., Liu, W., Leng, X., Song, C., ... & Yao, K. (2007). Enhancement of transfection efficiency for HeLa cells via incorporating arginine moiety into chitosan. *Chinese Science Bulletin*, 52(23), 3207-3215
- ✓ Yoksan, R., & Akashi, M. (2009). Low molecular weight chitosan-gl-phenylalanine: preparation, characterization, and complex formation with DNA. *Carbohydrate polymers*, 75(1), 95-103
- ✓ Yu, H., Deng, C., Tian, H., Lu, T., Chen, X., & Jing, X. (2011). Chemo-Physical and Biological Evaluation of Poly (L-lysine)-Grafted Chitosan Copolymers Used for Highly Efficient Gene Delivery. *Macromolecular bioscience*, 11(3), 352-361.
- ✓ Xie, W., Xu, P., Liu, Q., & Xue, J. (2002). Graft-copolymerization of methylacrylic acid onto hydroxypropyl chitosan. *Polymer Bulletin*, 49, 47-54.
- ✓ Jeon, Y. J., & Kim, S. K. (2001). Effect of antimicrobial activity by chitosan oligosaccharide N-conjugated with asparagine. *Journal of Microbiology and Biotechnology*, 11(2), 281-286
- ✓ Wang, B. L., Wang, J. L., Li, D. D., Ren, K. F., & Ji, J. (2012). Chitosan/poly (vinyl pyrrolidone) coatings improve the antibacterial properties of poly (ethylene terephthalate). *Applied surface science*, 258(20), 7801-7808.
- ✓ Raorane, C. J., Shastri, D., Parveen, A. S., Haldhar, R., Raj, V., & Kim, S. C. (2022). Grafted Chitosan-Hyaluronic Acid (CS-g-poly (MA-co-AN) HA) Complex Inhibits Fluconazole-Resistant Candida albicans Biofilm Formation. *Antibiotics*, 11(7), 950.)
- ✓ Ailincui, D., Marin, L., Morariu, S., Mares, M., Bostanaru, A. C., Pinteala, M., ... & Barboiu, M. (2016). Dual crosslinked imino boronate-chitosan hydrogels with strong antifungal activity against Candida planktonic yeasts and biofilms. *Carbohydrate Polymers*, 152, 306-316

- ✓ Pinto, E. P., Tavares, W. D. S., Matos, R. S., Ferreira, A. M., Menezes, R. P., da Costa, M. E. H., ... & Zamora, R. R. M. (2018). Influence of low and high glycerol concentrations on wettability and flexibility of chitosan biofilms. *Quimica Nova*, *41*, 1109-1116.
- ✓ Jin, X., Wang, J., & Bai, J. (2009). Synthesis and antimicrobial activity of the Schiff base from chitosan and citral. *Carbohydrate research*, *344*(6), 825-829
- ✓ Singh, D. K., & Ray, A. R. (1998). Characterization of grafted chitosan films. *Carbohydrate polymers*, *36*(2-3), 251-255.
- ✓ Hernandez-Montelongo, J., Lucchesi, E. G., Gonzalez, I., Macedo, W. A. D. A., Nascimento, V. F., Moraes, A. M., ... & Cotta, M. A. (2016). Hyaluronan/chitosan nanofilms assembled layer-by-layer and their antibacterial effect: A study using *Staphylococcus aureus* and *Pseudomonas aeruginosa*. *Colloids and Surfaces B: Biointerfaces*, *141*, 499-506.
- ✓ Kandile, N. G., & Mohamed, H. M. (2021). New chitosan derivatives inspired on heterocyclic anhydride of potential bioactive for medical applications. *International Journal of Biological Macromolecules*, *182*, 1543-1553.
- ✓ Umar, A., Naim, A. A., & Sanagi, M. M. (2014). Synthesis and characterization of chitosan grafted with polystyrene using ammonium persulfate initiator. *Materials Letters*, *124*, 12-14.
- ✓ Yokoyama, A., Yamamoto, S., Kawasaki, T., Kohgo, T., & Nakasu, M. (2002). Development of calcium phosphate cement using chitosan and citric acid for bone substitute materials. *Biomaterials*, *23*(4), 1091-1101.
- ✓ Parker, A. C., Beenken, K. E., Jennings, J. A., Hittle, L., Shirtliff, M. E., Bumgardner, J. D., ... & Haggard, W. O. (2015). Characterization of local delivery with amphotericin B and vancomycin from modified chitosan sponges and functional biofilm prevention evaluation. *Journal of Orthopaedic Research*, *33*(3), 439-447.
- ✓ Carlson, R. P., Taffs, R., Davison, W. M., & Stewart, P. S. (2008). Anti-biofilm properties of chitosan-coated surfaces. *Journal of Biomaterials Science, Polymer Edition*, *19*(8), 1035-1046.
- ✓ Tang, H., Zhang, P., Kieft, T. L., Ryan, S. J., Baker, S. M., Wiesmann, W. P., & Rogelj, S. (2010). Antibacterial action of a novel functionalized chitosan-arginine against Gram-negative bacteria. *Acta Biomaterialia* *6*(7), 2562-2571.
- ✓ Cobrado, L., Azevedo, M. M., Silva-Dias, A., Ramos, J. P., Pina-Vaz, C., & Rodrigues, A. G. (2012). Cerium, chitosan and hamamelitannin as novel biofilm inhibitors? *Journal of Antimicrobial Chemotherapy*, *67*(5), 1159-1162
- ✓ Miles, K. B., Ball, R. L., & Matthew, H. W. T. (2016). Chitosan films with improved tensile strength and toughness from N-acetyl-cysteine mediated disulfide bonds. *Carbohydrate polymers*, *139*, 1-9.
- ✓ Adnik, U., Zemljic, L. F., Plohl, O., Pérez, L., Trček, J., Bračić, M., & Mohan, T. (2021). Bioactive Functional Nanolayers of Chitosan–Lysine Surfactant with Single-and Mixed-

Protein-Repellent and Antibiofilm Properties for Medical Implants. *ACS Applied Materials & Interfaces*, 13(20), 23352-23368.

- ✓ Vishu Kumar, A. B., Varadaraj, M. C., Gowda, L. R., & Tharanathan, R. N. (2005). Characterization of chito-oligosaccharides prepared by chitosanolytic with the aid of papain and Pronase, and their bactericidal action against *Bacillus cereus* and *Escherichia coli*. *Biochemical Journal*, 391(2), 167-175.
- ✓ Liu, Y., & Kim, H. I. (2012). Characterization and antibacterial properties of genipin-crosslinked chitosan/poly (ethylene glycol)/ZnO/Ag nanocomposites. *Carbohydrate polymers*, 89(1), 111-116.
- ✓ Yu, Z., Rao, G., Wei, Y., Yu, J., Wu, S., & Fang, Y. (2019). Preparation, characterization, and antibacterial properties of biofilms comprising chitosan and ϵ -polylysine. *International journal of biological macromolecules*, 141, 545-552.
- ✓ Hao, X., Yan, W., Yang, J., Bai, Y., Qian, H., Lou, Y., ... & Zhang, D. (2022). Matrine@chitosan-D-proline nanocapsules as antifouling agents with antibacterial properties and biofilm dispersibility in the marine environment. *Frontiers in Microbiology*, 13.
- ✓ Kumar, A. B. V., Varadaraj, M. C., Gowda, L. R., & Tharanathan, R. N. (2007). Low molecular weight chitosans—preparation with the aid of pronase, characterization and their bactericidal activity towards *Bacillus cereus* and *Escherichia coli*. *Biochimica et Biophysica Acta (BBA)-General Subjects*, 1770(4), 495-505.
- ✓ Huang, N. P., Michel, R., Voros, J., Textor, M., Hofer, R., Rossi, A., ... & Spencer, N. D. (2001). Poly (L-lysine)-g-poly (ethylene glycol) layers on metal oxide surfaces: surface-analytical characterization and resistance to serum and fibrinogen adsorption. *Langmuir*, 17(2), 489-498.
- ✓ Bulwan, M., Wójcik, K., Zapotoczny, S., & Nowakowska, M. (2012). Chitosan-based ultrathin films as antifouling, anticoagulant and antibacterial protective coatings. *Journal of Biomaterials Science, Polymer Edition*, 23(15), 1963-1980.
- ✓ Wang, Y., Han, Q., Wang, Y., Qin, D., Luo, Q., & Zhang, H. (2020). Self-assembly, rheological properties and antioxidant activities of chitosan grafted with tryptophan and phenylalanine. *Colloids and Surfaces A: Physicochemical and Engineering Aspects*, 597, 124763.
- ✓ Gotman, I. (1997). Characteristics of metals used in implants. *Journal of endourology*, 11(6), 383-389.